ICING HAZARD LEVEL

Final Report 2011-2012

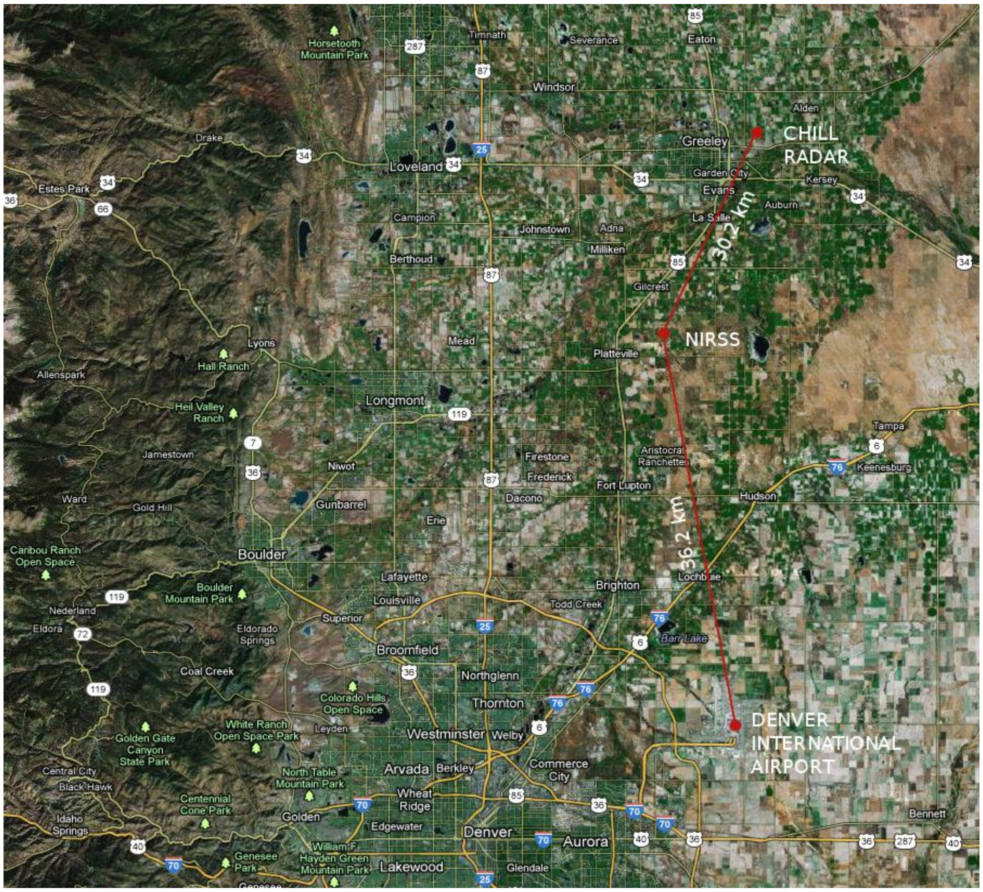

Prepared for: MIT Lincoln Laboratories

By: David Albo, Scott Ellis, David Serke, Andrew Weekley, Dan Adriaansen, Christopher Johnston, Marcia K. Politovich, Mike Dixon and John C. Hubbert

Scientific Lead: John C. Hubbert

National Center for Atmospheric Research
Research Applications Laboratory

10 February 2012

Executive Summary

This is the Final Report of the Icing Hazard Level (IHL) activities performed by NCAR for MIT Lincoln Laboratory for 2011/12. It is a continuation of the IHL work performed in 2010 and reported in “Icing Hazard Level Detection: Final Report” by NCAR for Lincoln Laboratory. The task is to develop an Icing Hazard Level Algorithm (IHLA) that utilizes dual-polarization radar data and output from an operational numerical weather prediction model. This work is motivated by the upcoming dual-polarization upgrade to the NEXRAD network. The starting point of this effort was based on existing algorithms for freezing level detection, freezing drizzle detection and particle type identification. Additionally, the IHLA relies on the extensive knowledge base at NCAR acquired from the development of the icing diagnosis and detection methods. Information about the above-listed algorithms can be found in the 2010 IHL Report.

In 2011/12 a major effort was the gathering of additional radar data sets for further development of the IHLA. As part of this effort, NASA Glenn Research deployed their NIRSS (NASA Icing Remote Sensing System) at the NOAA Platteville, CO field site from December 2010 to June 2011. NIRSS has been shown to have good skill in discriminating and quantifying cloud liquid water and thus, for this project, was used as verification for the IHLA. The Platteville site is 30 km west-southwest of the CSU-CHILL S-band dual-polarization radar, located just north of Greeley, CO. The Platteville site is also located under one of the Denver International Airport (DIA) flight path corridors so that pilot reports are frequently available for verification of the IHLA. Twenty CSU-CHILL data sets were used in this report for IHLA development. A subcontract was awarded to CSU for their assistance in this project; CSU-CHILL staff was instrumental in the gathering of the radar data.

The IHLA from 2010 was developed in several different programming environments. A major part of the 2011/12 work was to unify these codes into a single programming environment.

The fuzzy logic used in the IHLA is further developed, discussed and documented here. Though far from an operational algorithm, this preliminary design shows promise. More dual-polarization data sets from icing condition environments should be collected to help refine and tune a more robust and verifiable IHLA.

Contents

1. Introduction

The detection of super cooled liquid water (SLW), and thus inflight icing conditions, by radar alone is difficult. The liquid drops are typically quite small (< 50 μm in diameter) and have correspondingly low reflectivity values. If the drops are mixed with ice crystals (i.e., mixed-phase conditions), the ice crystals can dominate the backscatter radar signatures due to their generally larger size. Additionally, irregular, randomly-oriented ice crystals and small liquid drops are both characterized by Z_{dr} (differential reflectivity) and K_{dp} (specific differential phase) near zero. Thus, discrimination of SLW (a possible icing hazard) and ice crystals is challenging.

Identification of supercooled liquid water using dual-polarimetric radar has been investigated for some time. One of these efforts was the development of the PID (Particle IDentification) fuzzy logic algorithm (Vivekanandan et al. 1999), based on fuzzy logic membership functions for various hydrometeor types. The PID researchers found that the polarimetric membership functions for supercooled liquid water completely overlapped with irregular-shaped ice, i.e., ice that is characterized by zero average Z_{dr} and zero average K_{dp}. Thus, even with the benefit of these hydrometeor shape-based radar parameters, ambiguity remained. The fuzzy logic used by PID to distinguish these particle classes is based on radar variables at one range gate or resolution volume.

More recently, Ikeda et al. (2009) developed a freezing drizzle detection algorithm for the NEXRAD radars that was based in large part on various metrics of spatial texture of reflectivity. They found that clouds producing drizzle at the surface exhibited smoother reflectivity textures than those producing snow. Thus, they were able to discriminate between these two particle classes at least for 70% of their observed drizzle cases. Plummer et al. (2010) have recently made similar type discriminations from comparisons of aircraft observations (particle probes) and S-band (NSF's S-Pol) radar data from a field campaign in northern Italy. They examined histograms of Z_{dr} and K_{dp} and concluded that

1) the mean values of K_{dp} and Z_{dr} were greater in regions of ice-only as compared to mixed-phase (supercooled liquid and ice particles); and
2) the variance of Z_{dr} and K_{dp} were also greater in regions of ice-only as compared to mixed-phase.

Thus, these newer studies strengthened the idea that radar data, and in particular dual-polarization radar data, can offer skill in identifying aircraft icing conditions.

The concepts presented by these two published studies were investigated and reported in NCAR's 2010 Icing Hazard Level Detection, Final Report. In this report we further develop and test these ideas with the addition of a modified PID.

2. Icing Hazard Level Algorithm

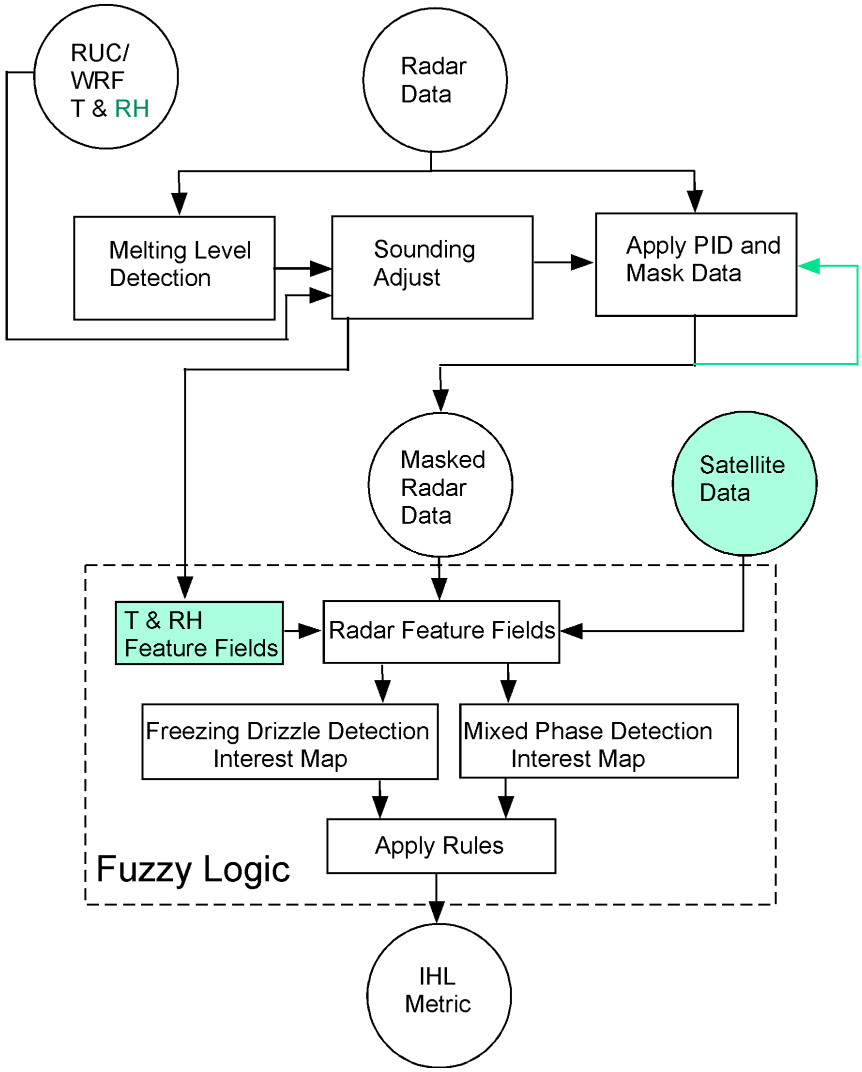

Figure 1: High-level diagram of the IHLA. Green-shaded features are not used in the current IHLA but the architecture allows for these in future versions.

The inputs to IHLA are radar and Numerical Weather Prediction (NWP) model data (Fig. 1). The Rapid Update Cycle (RUC) model was used in algorithm development; this will be replaced in spring 2012 with the Weather Research and Forecast Rapid Refresh (WRF-RAP) model. The Open Radar Products Generator (ORPG) currently ingests temperature and relative humidity profiles from the NWP model. The current IHLA only uses temperature. NCAR staff examined differences between RUC and WRF-RAP outputs to prepare their Current and Forecast Icing Product (CIP and FIP) algorithms for the transition. Significant differences were not found in the temperature field. When input into the IHLA, the radar data are assumed to have been processed with an algorithm such as CMD (Clutter Mitigation Decision) and a clutter filter such as GMAP (Gaussian Model Adaptive Processing), which is used by NEXRAD.

2.1 IHLA Description

2.1.1 Overview

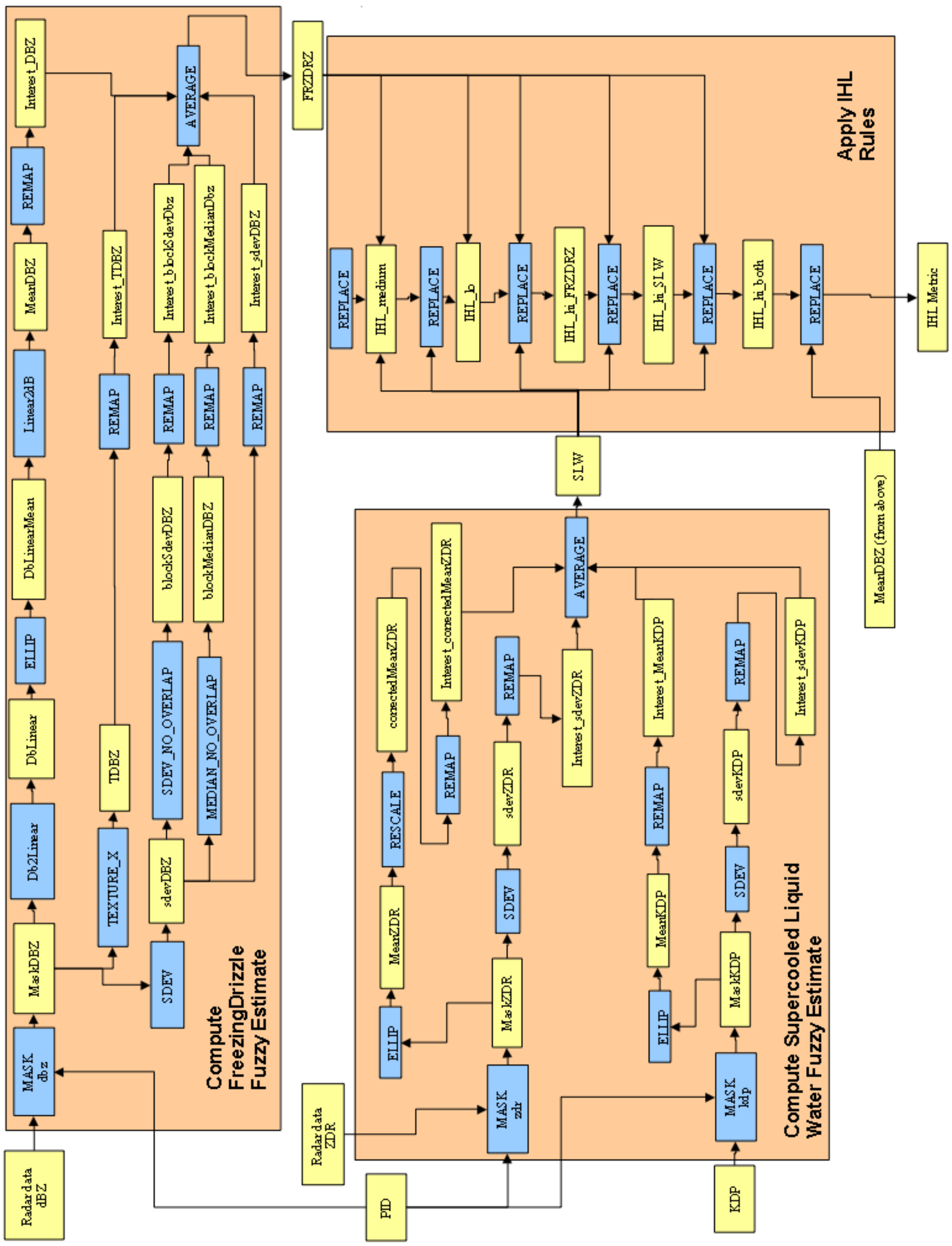

Figure 2: Detailed flow diagram for the IHLA. The freezing drizzle (MNDDA) algorithm is at the top; the supercooled liquid (SLWA) algorithm is at bottom left; the final IHLA calculation is at bottom right. This diagram is available online at http://rap.ucar.edu/projects/IHL/IHLAlgorithm/Page1.html

The IHL algorithm works with quality-controlled polarized S-band netCDF data files that have been masked to utilize only certain particle types. Statistical fields based on these moment fields are calculated and used within two 'meta-algorithms' that are described in detail in the following section. The two meta-algorithms are a modified version of the Ikeda et al. (2009)-based NEXRAD Drizzle Detection Algorithm (MNDDA, referred to as FRZDRZ within IHL) and a Supercooled Liquid Water Algorithm (SLWA) based on Plummer et al. (2010). It is important to keep in mind that there are vastly different microphysical cloud processes that result in the type of in-flight icing conditions described by these investigators. A radar-based icing detection algorithm needs to have the flexibility to differentiate these conditions based on the radar signatures induced by the atmospheric phenomena. The meta-algorithms and their subsequent usage in the resulting IHL algorithm are detailed below.

2.1.2 FZLA algorithm

The FreeZing Level Algorithm (FZLA) is described in detail in the NCAR 2010 IHL Final Report and here only the algorithm summary is repeated for convenience. The entire processing sequence goes as follows:

For each radar volume
    For each elevation angle scan
        double ring filter of ρ_{hv}
        double ring filter of dBZ
        double ring filter of Z_{dr}
        max combine
        smooth
        clump
    build a two-dimensional Histogram of percent clumped
    adjust for quality
    adjust for scan related consistency
    determine z, Q for this volume by doing ridge-finding
    end
end

Details are shown in Fig. 3. Specific elevation angles are given in Fig. 3, however, the process is executed on all available angles. The process is the same for all four; the outputs are combined, adjusted for data quality values, and a final histogram is produced at the end which is used to estimate the height of the freezing level. Technically speaking, this is a melting level, or 0^{o}C level rather than a freezing level, but the historic terminology in the community is for it to be referred to as a freezing level. In the spirit of minimizing confusion, we refer to it as freezing level.

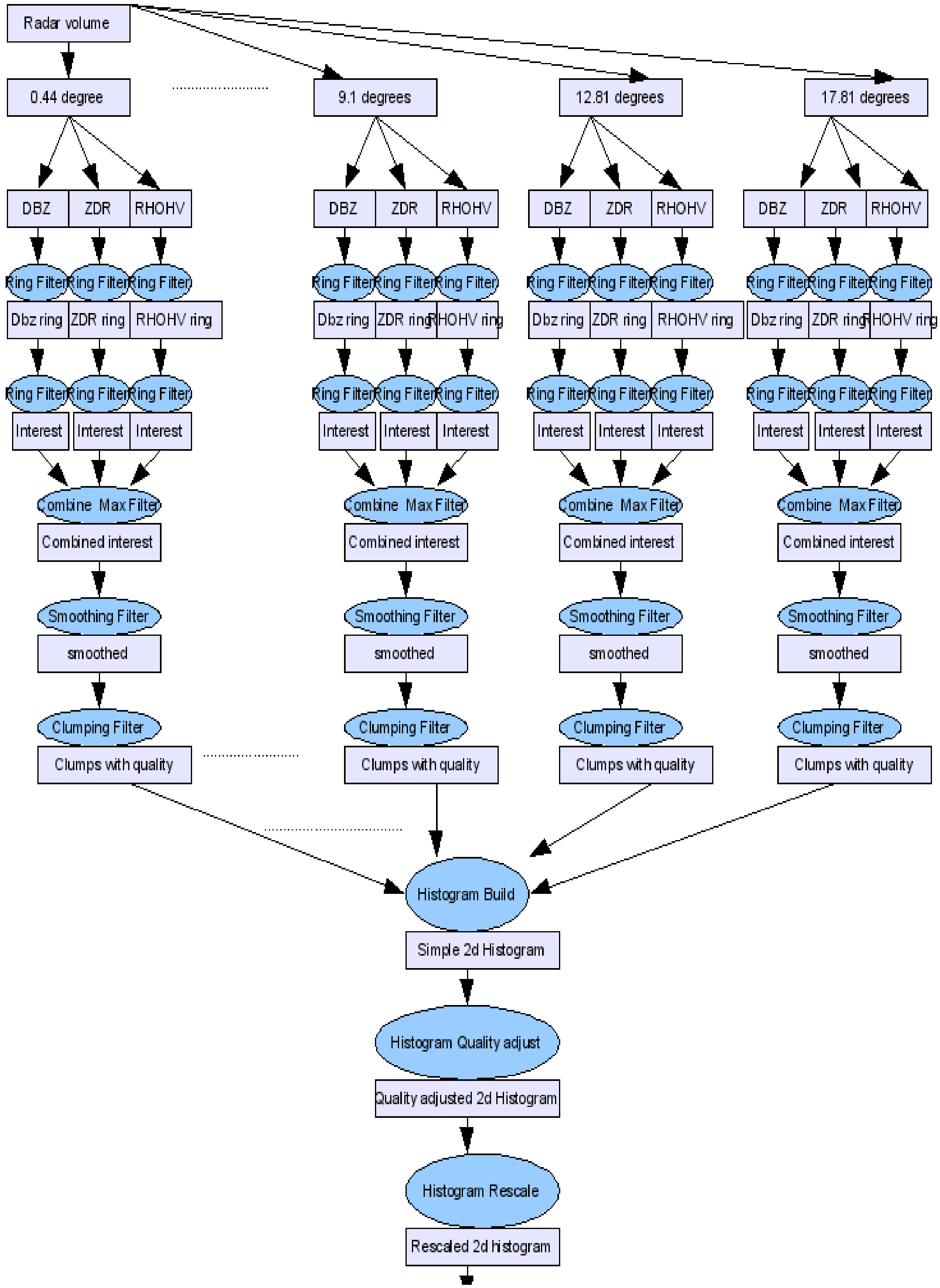

Figure 3: Flow diagram for the FZLA.

2.1.3 MNDDA meta-algorithm

The NEXRAD Drizzle Detection Algorithm (NDDA) was developed by Ikeda et al. (2009) to detect freezing drizzle using NEXRAD reflectivity data. A detailed description of the algorithm, results and scientific motivation can be found in Ikeda et al.(2008) but a summary of the findings are discussed here. The algorithm calculates numerous statistical measures (or feature fields) and uses fuzzy logic to convert these measures into scores; the individual scores are then combined into a single final score. If the final score is above a specific threshold, freezing drizzle is inferred to be present in the scan. The statistical measures calculated are the median reflectivity, the global standard deviation of the reflectivity, the median of the local standard deviation of the reflectivity, the standard variation of the local standard deviation of the reflectivity, and the median reflectivity of the local texture. Note the statistical measures are single values for each range gate calculated over a specified domain. The NDDA uses two domains: near (15 km) and far (100 km). Consequently, ten scores are combined to determine the final overall score. To implement the algorithm one needs to calculate the median and standard deviation of a 2-D field over a specified range and azimuth domain, calculate a standard deviation over a local range and azimuth region, and calculate a texture over a local range and azimuth region. Finally, the output statistics must be remapped into scores using piecewise linear functions (see Ikeda et al., 2008).

The NDDA algorithm was designed to identify freezing drizzle at the surface. Therefore modifications were made to the NDDA algorithm to extend the identification region above the surface in order to be applicable for aircraft icing. The Modified NDDA (MNDDA) is similar to the NDDA with the following changes. The statistical measures of the near domain computed over 15-km range were computed over successive 15-km rings extending in range from the radar and using scans of multiple elevation angles. This extended the freezing drizzle classification above the surface to altitudes useful for aircraft icing detection.

In the original NDDA the 100-km domain was used as a proxy for the vertical structure. However for the MNDDA multiple elevation angles are used with the 15-km domain thus obtaining vertical structure information across a smaller horizontal extent. The 100-km domain was not used in the MNDDA.

A new feature field, texture of dBZ (TDBZ), was added to the MNDDA. The texture is mean of the gate-to-gate difference of reflectivity in range. Therefore there are six feature fields contributing to the MNDDA output. The TDBZ values are expected to be lower in freezing drizzle than in ice.

The membership functions for the MNDDA as presented in this report are shown in Fig. 4. The processing needed to calculate the final MNDDA score (assuming the PID has already been implemented and applied to the input reflectivity data) is shown in Fig. 1.

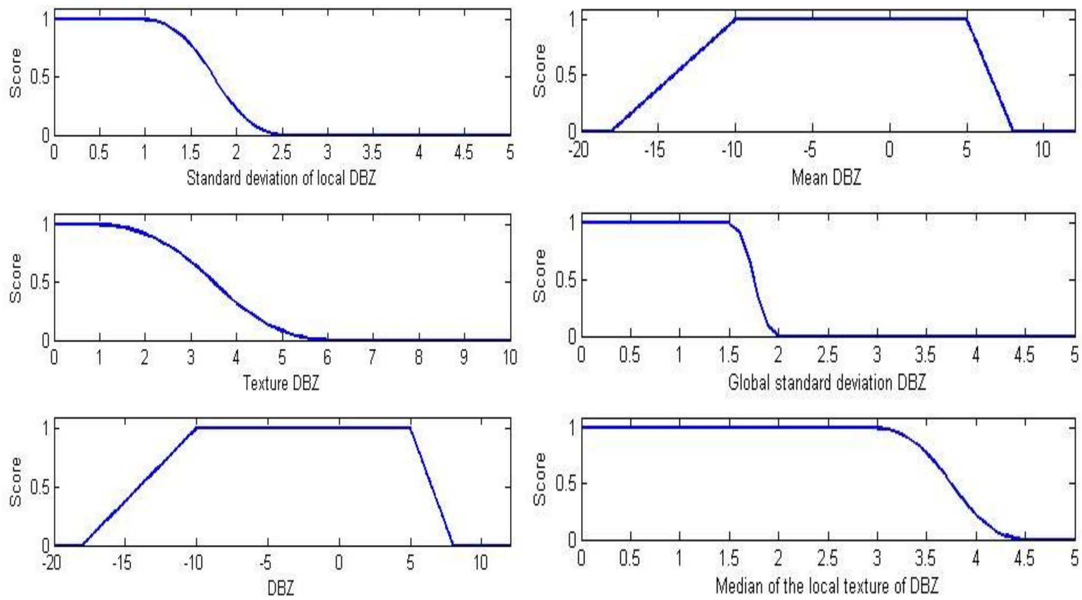

Figure 4: MNDDA membership functions.

2.1.4 PID

The Particle Identification algorithm (PID) is described in detail by Vivekanandan et al. (1999) but pertinent information will be discussed here.

Table 1: PID Output Fields

Field name	**Field units**	**Description**
K_{dp}	^{o}/km	K_{dp} value
Particle ID	*	Primary particle classification
Particle Interest	Value from 0-1	Interest score for the most likely particle type
Particle ID #2	*	Secondary particle classification
Particle Interest #2	Value from 0-1	Interest score for the second most likely particle type
Z_{dr} for PID	dB	Smoothed Z_{dr} values used for particle identification interest calculations
K_{dp} for PID	^{o}/km	Smoothed K_{dp} values used for particle identification interest calculations
Temperature for PID	C	Sounding temperature values used for particle identification interest calculations

* Particle types are indicated by a number as 1=cloud, 2=drizzle, 3=light rain, 4=moderate rain, 5=heavy rain, 6=hail,7= rain/hail mixture, 8=graupel small hail, 9=graupel rain, 10=dry snow, 11=wet snow, 12=ice crystals, 13=irregular ice crystals, 14=supercooled liquid water, 15=flying insects, 16=second trip, and 17=ground clutter.

The PID uses reflectivity, K_{dp} , correlation coefficient (ρ_{hv}), and Z_{dr} from the radar and temperature from an available atmospheric sounding or model output to evaluate the most likely hydrometeor type present in a radar volume (range gate within a single beam). PID uses fuzzy logic membership functions to describe the relevance of the radar parameters to a given hydrometeor type. The output is a series of values related to the chosen particle type, as listed in Table 1. The downstream algorithms use the PID particle types as a mask, allowing IHL estimation only where relevant types are found.

It has been noted by several researchers that hydrometeor identification algorithms such as the PID have poor performance in winter storms (Plummer et al., 2010; Lakshmanan et al., 2010), in particular for discriminating SLW from ice. Winter hydrometeor identification is becoming a more active area of research, especially with the NEXRAD dual-polarization upgrades taking place. The current IHLA uses PID output in a very rudimentary way so that details of the exact particle type identified by the algorithm are not critical. However, in future IHL work, the PID could be updated to improve winter performance through direct studies or collaborations with other programs and organizations doing similar research.

2.1.5 SLWA meta-algorithm

Plummer et al. (2010) examined the utility of dual-polarization variables to discriminate SLW from ice-only conditions. Their findings were adapted into an algorithm (SLWA) by NCAR researchers and applied to the CSU-CHILL data. The feature fields used in SLWA are computed over a local area and include the mean of Z_{dr}, standard deviation of Z_{dr}, mean of K_{dp} and the standard deviation of K_{dp}. Membership functions similar to those described in the MNDDA were designed and applied to produce interest values (Fig. 5). Next, the four interest values were combined into a weighted sum and normalized to obtain an output from 0 to 1, with 0 suggesting no likelihood of icing and 1 a high likelihood of icing. The SLWA identification from this algorithm generally indicates a high possibility of icing at similar times that NIRSS indicates high in-flight icing hazard for the data of the 2010/2011 field campaign. These results are also generally consistent with the pilot reports of icing. The overall flow of the SLWA is shown in Fig. 2.

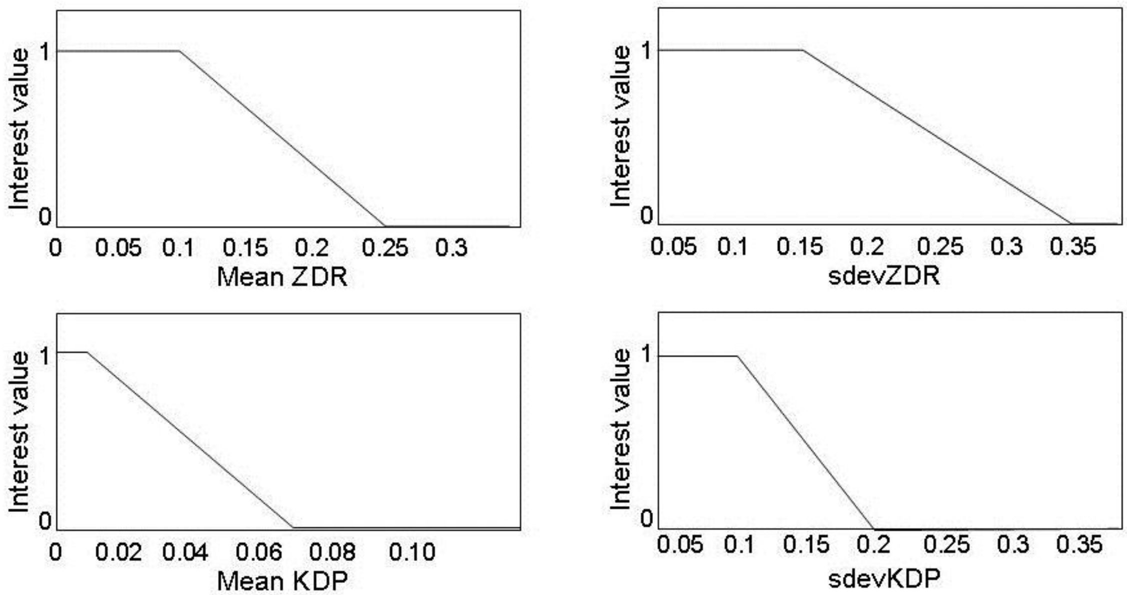

Figure 5: Membership functions within the SLWA for mean (left) and standard deviation (right) of Z_{dr} (top) and K_{dp} (bottom).

2.1.5 Final IHL output

The final IHL output is a combination of the resulting interest fields from the two meta-algorithms MNDDA and SLWA. The icing hazard values are sorted into various categories, and each category is assigned an IHL value as defined in Table 2.

Table 2: Final IHL Output

Category	Name	Description	Value	Icing
1	High SLW	SLWA output >0.55	1.0	Yes
2	High FZDZ	MNDDA output >0.70	0.7	Yes
3	Both high	Category 1 and 2 apply	0.8	Yes
4	Both low	SLWA and MNDDA output both <0.45	0.0	No
5	Below SNR	When mean dBZ < -31 dBZ	-0.1	Unknown
6	Both medium	Not categories 1 through 5	0.5	Maybe

The threshold values for these categories were determined by exhaustively analyzing all the available polarized research radar moment fields with respect to PIREP- and NIRSS-indicated hazard, and integrated liquid water (ILW) values at times of positive and negative icing during the 2010/2011 field campaign. The details of these case comparisons are discussed in the later sections of this report. Each category is assigned the following IHL value as listed in Table 2.

It is important to note that while the encoded IHL values for 'high SLW' (Cat 1), 'high FRZDRZ' (Cat 2) and 'both high' (Cat 3) are different, all three correspond to the IHL algorithm detecting the in-flight icing hazard as 'Yes'. The discrete nature of these three categories was preserved from the developers' version to the version delivered to MIT-LL so that other researchers can see when the meta-algorithms are warning on positive icing hazard. Also, future upgrades and case studies may warrant additional meta-algorithms, with which the furthering of the discrete nature of encoded positive icing can be easily tracked.

2.1.6 Temperature considerations

The IHL algorithm relies on a temperature profile from numerical weather model output that is closest to the radar location. Since more than one grid point in the numerical weather model domain exists within the radar domain it's possible that the closest grid point to the radar location may not always be the most representative. For example, different sectors of weather systems could simultaneously be impacting the radar domain leading to variations in not only freezing level (temperature) but the type of conditions conducive to icing as well. In these situations it may be more effective to classify certain regions of the radar domain in one manner, while using a different approach to icing diagnosis in another region. This would allow for the selection of a certain temperature profile in one region while using a different profile in another area thus improving the resulting icing diagnosis and representativeness of the temperature profile. Cases where conditions are relatively uniform and where conditions vary across the domain will be examined to try and identify the most intelligent method for selection of a temperature profile.

3. The 2010-2011 Field Campaign

In a collaborative effort with NASA, the NIRSS (NASA Icing Remote Sensing System) was brought from NASA Glenn Research Center in Cleveland, Ohio, to the Front Range of Colorado for the period of December 2010 to June 2011. NIRSS was deployed at the NOAA-owned Platteville, CO field site, which is close to the CSU-CHILL radar and is conveniently located under the flight path of aircraft arriving and departing from Denver International Airport (DEN, see Fig. 6 and title page photograph). NIRSS measurements and PIREPS were used to indicate whether or not icing conditions existed. Twice-daily meteorological balloon soundings from Denver and surface observations from the area were also used for case study analyses.

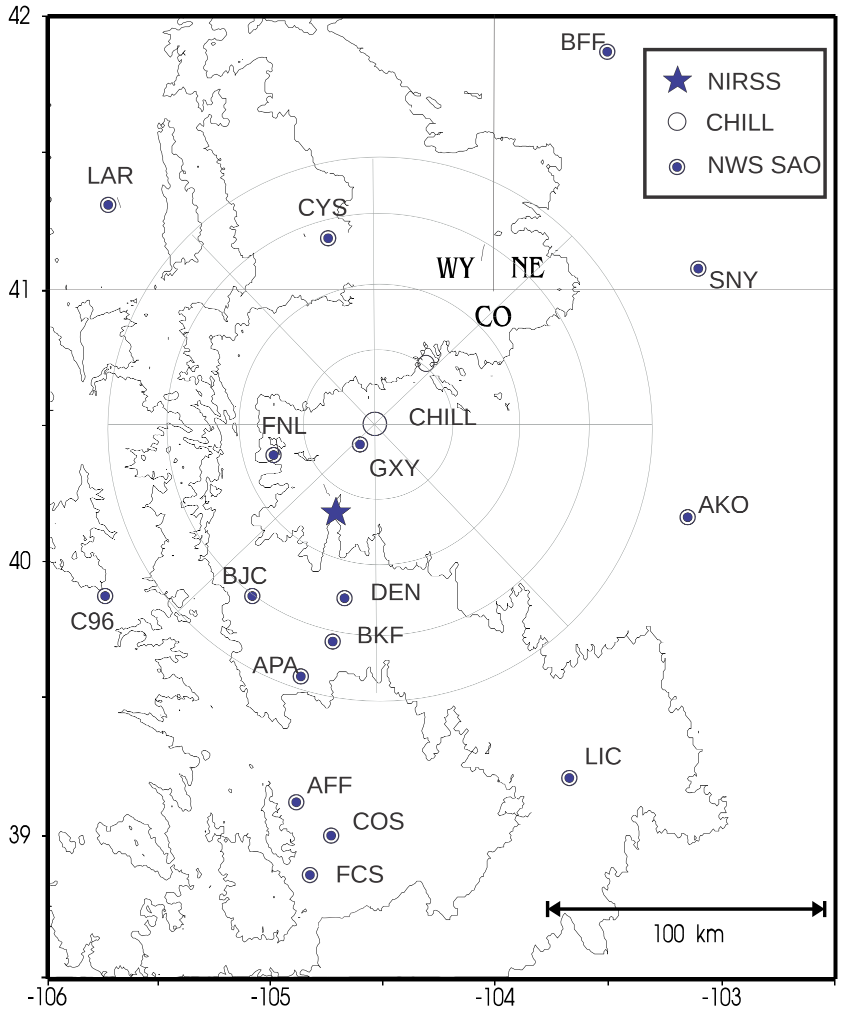

Figure 6: Map of the Front Range of Colorado, showing the location of CSU-CHILL, NIRSS and National Weather Service Surface Atmospheric Observations (NWS SAO). Range rings around CSU-CHILL are at 25-km intervals. Terrain contours start at 5,000 ft MSL with 2,000-ft increments.

3.1 CSU-CHILL

The Colorado State University – University of Chicago – Illinois State Water Survey (CSU-CHILL) National Radar Facility is fully described by Brunkow et al. (2000). CSU-CHILL is a transportable dual-polarization S-band (10-cm wavelength) radar system, with a 9-m parabolic dual-offset reflector antenna. The radar features dual Klystron transmitters driving each polarization channel. Each transmitter develops approximately 1 MW of power.

Figure 7: The CSU-CHILL research radar near Greeley, CO.

3.2 NIRSS

NIRSS consists of a vertically-pointing Doppler K_a-band radar, a multichannel microwave radiometer and a laser ceilometer (Fig. 8, Reehorst et al., 2006). A Radiometrics model 3000 multi-channel radiometer passively collects incoming microwave radiation at a number of channels in the K and V-bands of the electromagnetic spectrum (Solheim et al., 1998). The K-band lies within an atmospheric window and thus variations at specific frequencies within the band are due to variations in the amount of liquid and gaseous water. Different amounts of gaseous and liquid phase water cause the amount of microwave radiation received by the radiometer at frequencies within the K band to respond differently. Integrated liquid water (ILW) and integrated water vapor (IWV) are retrieved from 22.23 and 30.0 GHz channels as in Hogg et al. (1983). The instrument's V-band channels are on the shoulder of a major oxygen absorption feature, so that progressively varying frequencies from the peak of the absorption feature yields information on the atmospheric temperature further from the radiometer in range. This allows for the derivation of an atmospheric temperature profile. The temperature profile and ILW are ingested into an algorithm that combines the fields into an in-flight icing product. The vertical extent of cloud boundaries are provided by the ceilometer and K_a-band cloud radar. If cloud exists within the height range where icing temperatures exist, any liquid sensed by the radiometer is then distributed vertically with fuzzy logic, based on previous experience with years of research flights in icing conditions (Reehorst et al., 2005).

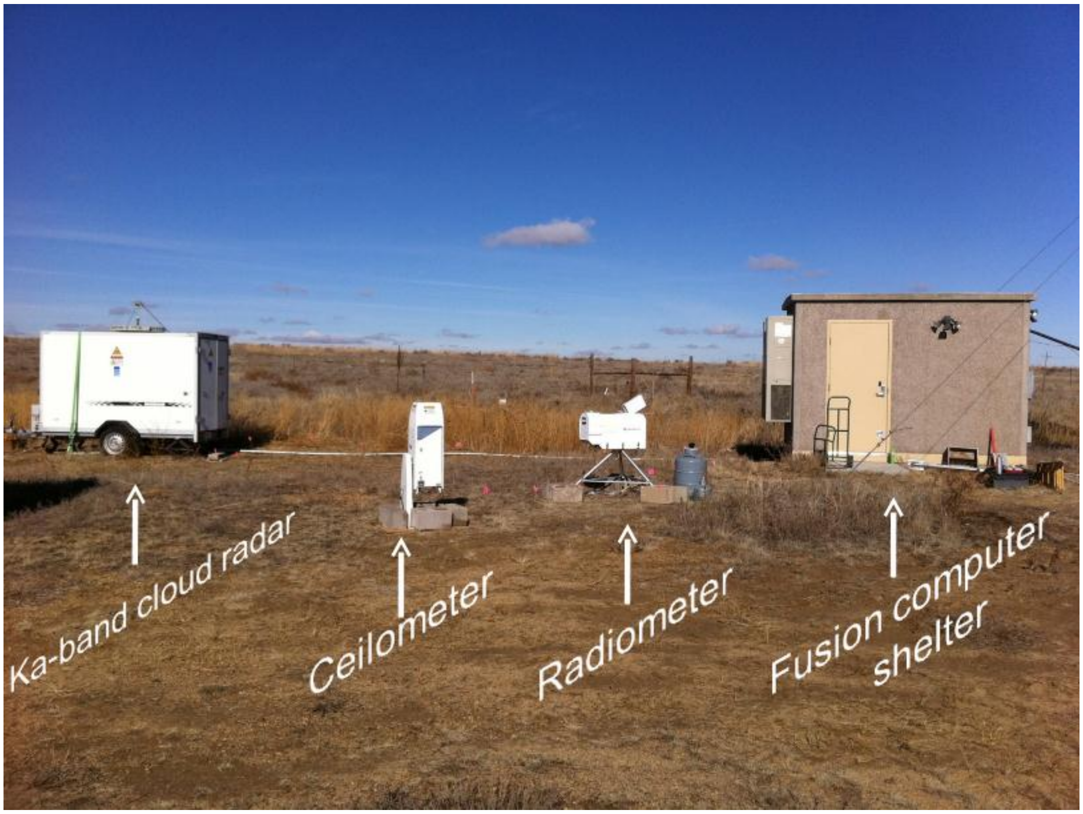

Figure 8: NIRSS components deployed at Platteville, CO.

NIRSS was located south of CSU-CHILL at an azimuth of ~195^o at a range of 30 km, in an unblocked region of the radar scan range.

3.3 PIREPs

A PIREP is a voice PIlot REport that is transmitted to ground staff at Air Route Traffic Control Centers, Terminal Radar Area Control Operations Centers, or Flight Service Stations, who subsequently code the report into a database. In-flight icing is one of many possible conditions that can be reported by pilots during flight. The existence of icing can be reported as 'no icing exists' or 'icing exists' with a severity of ‘trace’, ‘light’, ‘moderate’, ‘severe’ or ‘heavy’. Note that while definitions exist for pilot reporting of these icing categories, there are no meteorological definitions and, that “severe” and “heavy” categories are somewhat ambiguous. Over the course of the field campaign, over 350 icing PIREPs were reported within 50 km of NIRSS, 48 of which were within 25 km.

4. Experimental Data

4.1 Case Studies

CSU-CHILL and NIRSS collected twenty-two cases during the field experiment as listed in Table 3. Five of these will be discussed in detail in a later section. For all cases, data were checked for quality and archived. As shown in Table 3, quite a variety of weather types were sampled.

The NIRSS data provide a valuable independent measurement of SLW that can be used to verify the results of the IHLA. The analyses presented here will focus largely on evaluating the IHLA output in comparison to the NIRSS integrated liquid water (ILW). The comparisons with the radiometer have the advantage that the radiometer measurements are available at a known location for long periods of time enabling analysis in various conditions. The radiometer measurements have the disadvantage of measuring integrated liquid water (ILW) values, meaning we cannot know at what vertical levels the measured liquid is located. NIRSS does include algorithms that distribute the liquid water into the clouds according to cloud top temperature and reflectivity, however, this feature was not used in the comparisons. There is also no way to know if the liquid that is detected is mixed with ice particles.

The research and coded data processing modules that went into the IHLA hazard detection prototype were described above, as well as in in detail in the delivered documentation and in conference proceedings such as Ellis et al. (2011), Serke et al. (2011) and others. The purpose of this work is to describe the current IHLA product as it relates to synoptic and microphysical meteorological features of the captured case studies.

Data from nearly all the cases in Table 3 were included in the IHLA development. The data sets are available to researchers who should find them valuable for examining polarimetric radar response to various cloud environments; contact John Hubbert (hubbert@ucar.edu) for access. Brief descriptions of most cases are found in Appendix C.

The next section presents a discussion of data collected on 15-16 December 2010, followed by a side-by-side comparison of two cases. The first case has almost no ILW measured by NIRSS (non-icing case on 30 December 2010) and in the second, NIRSS indicates substantial ILW (icing case on 18 May 2011).

Table 3: Field Project Cases (highlighted cases are discussed in Section 4.2)

Year	Date	# CHILL Sweeps	PIREPs	Overview
2010	7 Dec	10	3	Weak stationary front
	15 Dec	70	2	Weak cold frontal passage
	16 Dec	17	0	“
	17 Dec	14	3	Weak upslope form cold air damming
	30 Dec	42	2	Intensifying synoptic low pressure creates upslope flow
	31 Dec	42	1	“
2011	9 Jan	2	3	Weak low pressure south of Denver creates weak upslope
	10 Jan	3	1	Inverted trough provides upslope wind component
	20 Jan	2	1	Mountain lee-side trough development provides upslope wind component
	31 Jan	6	4	Stationary front, cold air damming, weak upslope wind component
	8 Feb	2	2	Moderate cold frontal passage
	25 Feb	2	4	Stationary front provides occasional weak upslope wind component
	7 Mar	4	3	Strong cold front, significant upslope component
	29 Apr	2	1	Weak upslope behind weak developing surface low pressure
	4 May	4	2	Disorganized weak surface low pressure over central CO
	11 May	5	3	Instability behind weak cold frontal passage
	12 May	7	4	“
	14 May	2	2	Weak upslope
	18 May	20	2	Synoptic low develops south of Denver, jet interaction, weak convections
	19 May	11	3	Broad, weak surface low pressure over OK provides weak upslope
	24 May	1	1	Weak low pressure south of Denver creates weak upslope
	25 May	1	2	Weak inverted trough behind surface low pressure

4.1 Significant Cases

4.1.1 15-16 December 2010

Late on 15 December 2010, a strong arctic cold frontal crossed from north to south across the urban corridor of Colorado's Front Range. The reported surface temperature at KDEN dropped from 52^{o}F to 16^{o}F over a 15-h period (Fig. 9). The frontal passage occurred at about 2100 UTC on the 15th (Fig. 10), as suggested by tendencies in temperature and pressure and a shift in wind direction to the NE. There was a weak upslope wind component (easterly, toward the Front Range of the Rocky Mountains) for several hours before as well as after the frontal passage. Precipitation was only reported for a 1-h period at 0000 UTC on the 16th as light snow (Fig. 11). The 16 December 0000 UTC Denver sounding (Fig. 12) shows relatively dry air below cloudbase , which was at ~4000 ft AGL. The atmosphere was nearly saturated from 750 to 650 mb, with conditional instability to 550 mb. Freezing level at this time was ~1500 ft AGL.

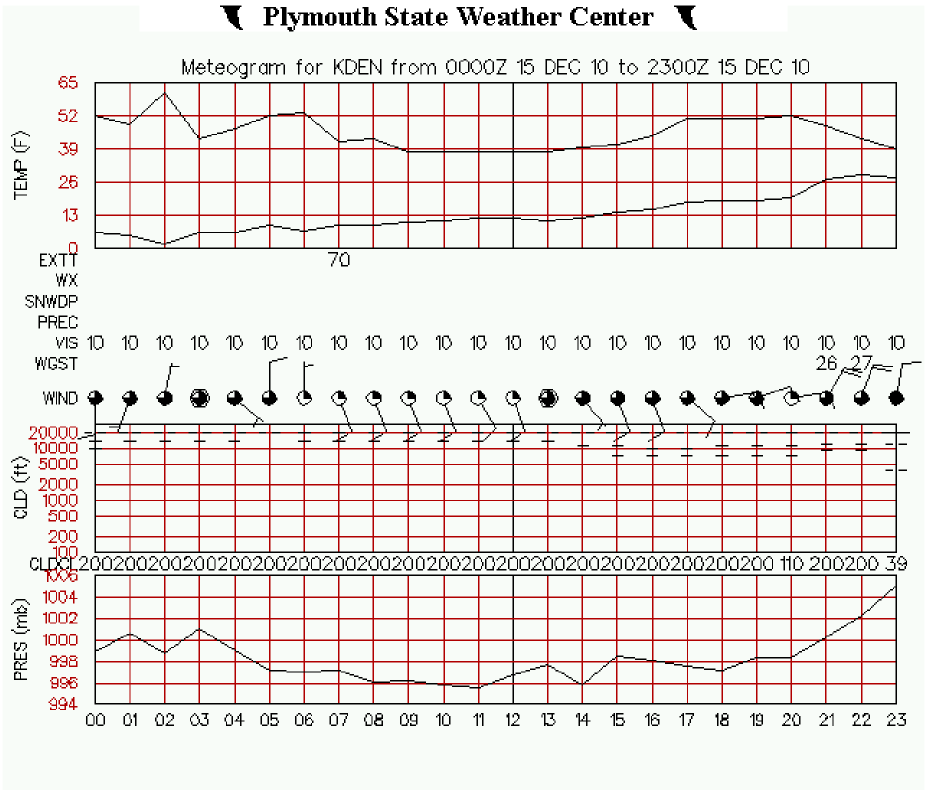

Figure 9: Meteogram of hourly surface weather conditions reported at KDEN from 0000 to 2300 UTC on 15 December 2010.

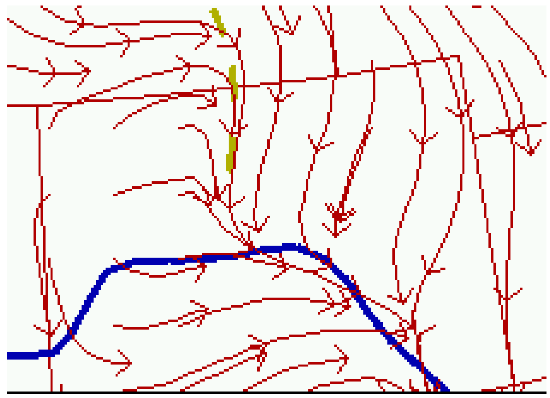

Figure 10: National Center for Environmental Prediction-analyzed surface fronts (blue=cold front) and surface streamlines (red arrows) at 2100 UTC on 15 December 2010.

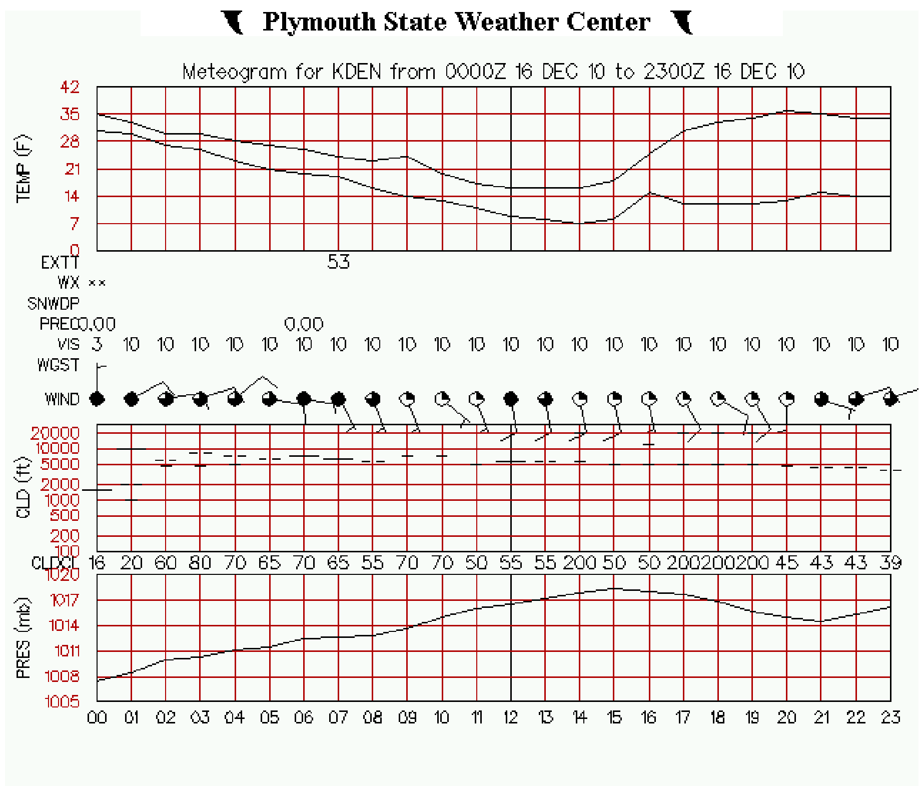

Figure 11: Meteogram of hourly surface weather conditions reported at Denver from 0000 to 2300 UTC on 16 December 2010.

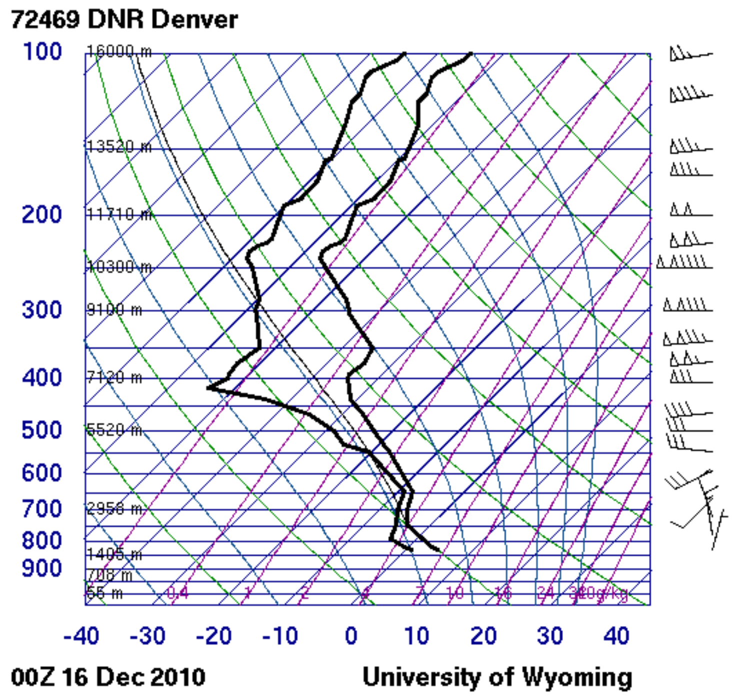

Figure 12: DENVER sounding at 0000 UTC on 16 December 2010.

Four hours prior to the NIRSS-detected icing condition over Platteville, a severe icing PIREP was reported over Cheyenne, WY. Later, two icing PIREPs were reported within 50 km of Platteville at 0040 and at 0100 UTC as the slow-moving front eventually pushed past DIA (~40 km SE of Platteville). These PIREPs occurred near the time of maximum ILW, (Fig. 13, black line). For this case, significant ILW, defined by values > 0.1 mm, only exist from 2350 UTC on the 15^{th} until about 0110 UTC on the 16th. It is this time period, during which positive icing PIREPs exist with significant ILW, that will be explored in more detail with the IHLA in the next few paragraphs.

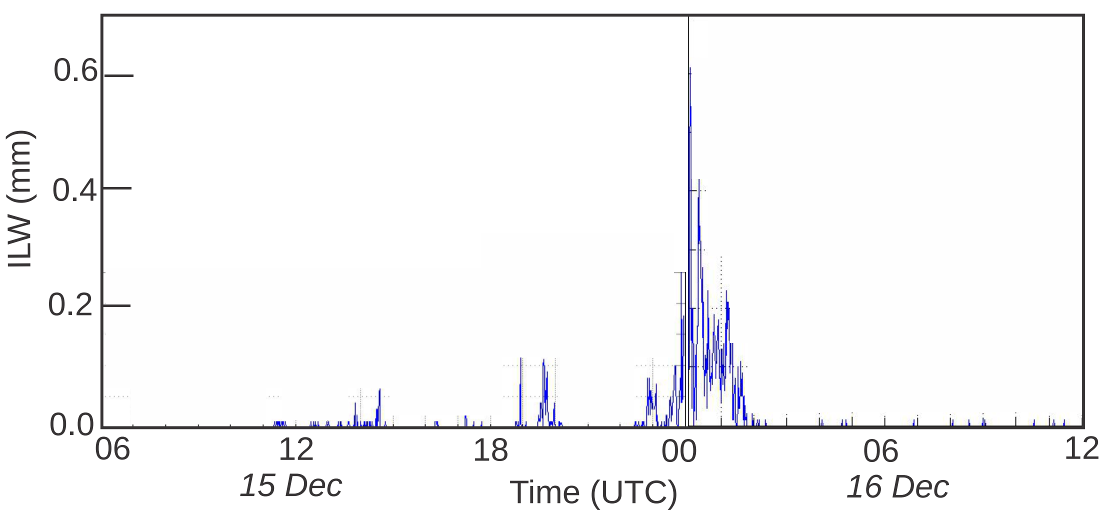

Figure 13: Time series of NIRSS radiometer ILW for 15 - 16 December 2010.

Figures 14-17 show derived IHLA icing hazard at two radar elevations for the same time. The upper is 4.5^{o} and the lower is 2.5^{o}. The 4.5^{o} angle is included in the discussion to represent a higher inclination yet still show derived values at ranges to 30 km, which is NIRSS' distance from CSU-CHILL. The 2.5^{o} angle is included in the discussion to represent more of a constant altitude plot in the area of interest while not being too highly influenced by ground clutter. IHLA output relies on the outputs of the Ikeda et al. (2009)-based freezing drizzle identification algorithm (MNDDA) and the Plummer et al. (2010)-based SLW algorithm (SLWA, both described in Section 2). IHLA values are -0.1 for areas with low signal-to-noise ratio, 0.0 for areas of low SLWA and MNDDA interest, 0.5 for areas of medium SLWA and MNDDA interest, 0.7 for areas of high MNDDA interest but not high SLWA interest, 0.8 for areas of high interest in both MNDDA and SLWA and 1.0 for areas of high SLW interest but not high MNDDA interest (see Table 2 in Section 2.1.5 for a list of these output values). Thus, areas with an IHL encoded value of 0.7 or greater should be considered as 'IHLA in-flight icing hazard equals yes'.

At 2251 UTC on 15 December, the leading edge of S-band reflectivity was progressing through the Platteville area but had not yet reached Denver. The NIRSS ILW value at this time (Fig. 13) was very low at <0.05 mm (Fig. 13). At both the upper and lower elevations shown (Fig. 14), IHL values were 0.0, corresponding to no detected icing. The horizontal scale of these icing features is on the order of several to tens of kilometers. It is of interest to note that the edges of return areas often become highlighted with a narrow edge one to two pixels wide of IHL=0.7, or high MNDDA interest. We consider this an artifact in the MNDDA 15-km standard deviation fields, and needs to be further explored and probably filtered in the future.

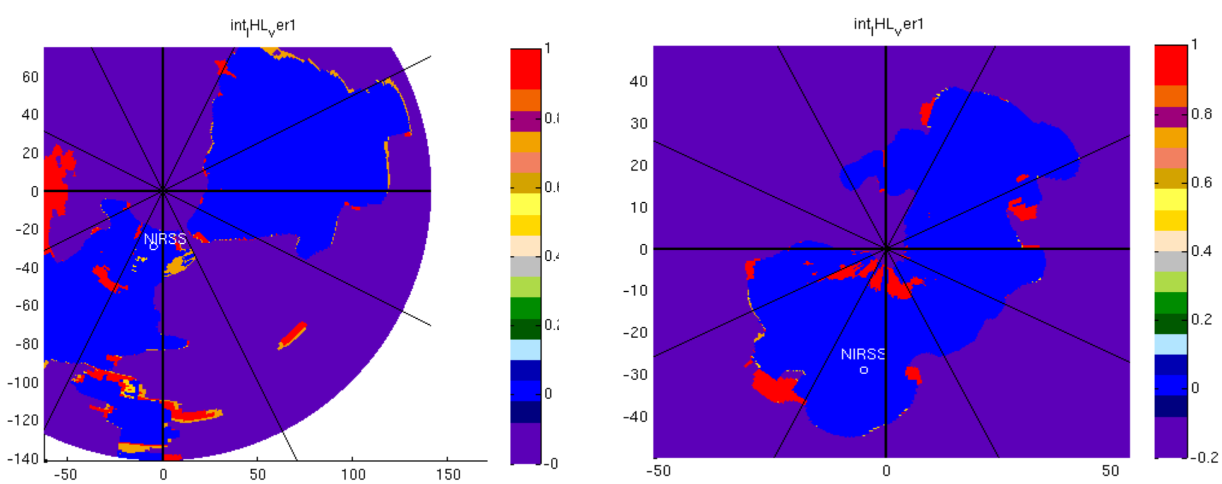

Figure 14: PPI plot of IHLA in-flight icing hazard index [unitless, scaled -0.1 to 1] for 2.5^{o} (left) and 4.5^{o} (right) elevations derived from CSU-CHILL radar at 2251 UTC on 15 December 2010.

By 2351 UTC on 15 December, the NIRSS radiometer was beginning to detect ILW >0.1 mm. Larger areas of IHL=yes values are located close to NIRSS in both the upper and lower elevations (Fig. 15), but the NIRSS profile is actually located in a gap in CSU-CHILL radar reflectivity. Pockets of higher IHL=yes values are seen near holes or discontinuities in return shapes, as noted in previous research (Serke et al., 2008).

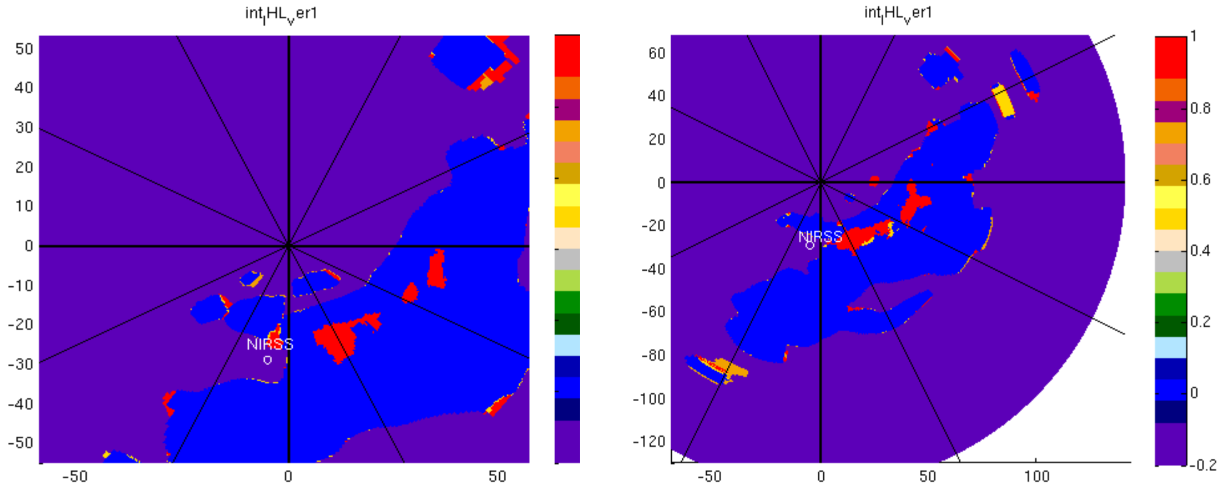

Figure 15: As for Fig. 14 except at 2351 UTC 15 December 2010.

At 0007 UTC 16 December, the ILW increased to near 0.2 mm (Fig. 13). With snow reported at the surface and temperatures decreasing steadily behind the front, this liquid was very likely supercooled. The lower-level elevation angle shows the lower-level CSU-CHILL echo several kilometers away from NIRSS (Fig. 16). Intricate banded features of high SLW interest (IHLA=1.0) exist parallel to the echo field and perpendicular to the direction of frontal motion. These features may be due to shear near the cloud tops (see DENVER sounding in Fig. 12) which can cause rolls or billows. During this case, cloud bands developed and 'blew-off' from west to east as the radar echo associated with the front progressed from north to south. The upper elevation angle once again shows areas of IHL=yes values near NIRSS, but the NIRSS site is essentially in an echo gap. By 0228 UTC, ILW had decreased to near zero (Fig. 5). Much of the CSU-CHILL radar echo had moved southward out of the radar's field of view, with a few scattered echo regions lingering east of NIRSS (Fig. 17). NIRSS was not near CSU-CHILL radar echo nor any area of IHL=yes values at this time.

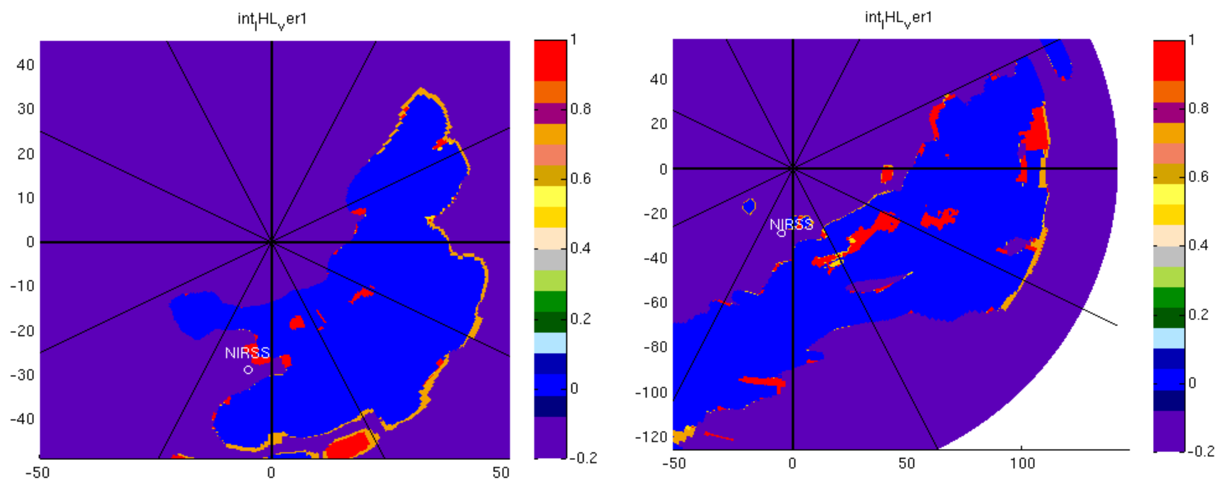

Figure 16: As for Fig. 14 except at 0007 UTC 16 December 2010.

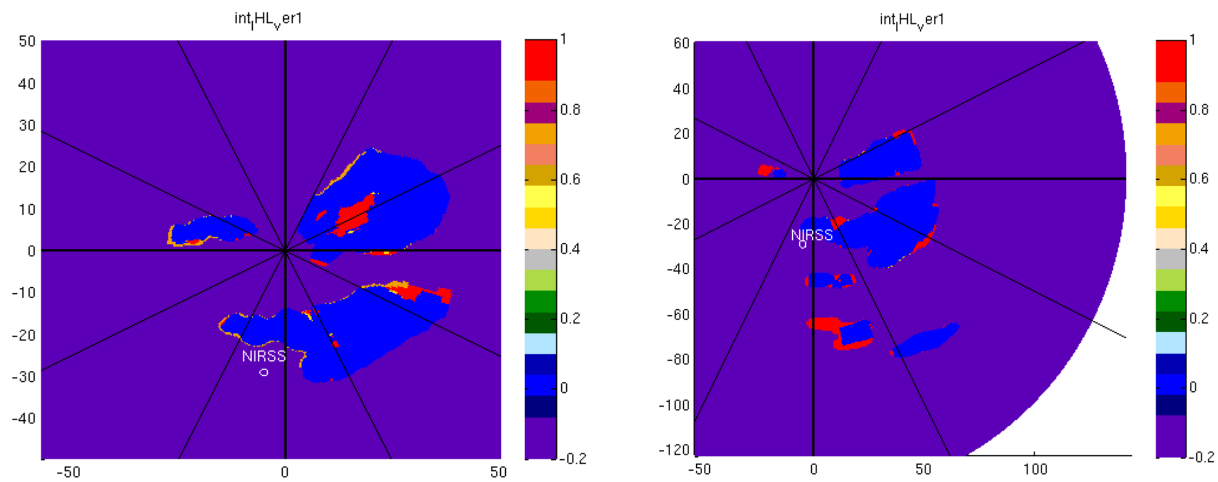

Figure 17: As for Fig. 14 except at 0228 UTC 16 December 2010.

One important lesson to take away from this case is that S-band radars, even finely-tuned research radars such as CSU-CHILL, are effectively precipitation radars and not cloud radars. Cloud-sized drop, considered as those with diameters <50 μm, are often not large enough to be detectable by these radars. Many previous studies have shown that small-drop only profiles can have much higher liquid water content and ILW values than those with larger drop profiles such as rain or drizzle due to much higher number concentrations of the smaller drops. A recent study by Johnston et al. (2012) showed that up to a third of icing events at Cleveland, OH over a three-year period had multiple cloud layers, where higher layers consisted of small particles that could not be detected by S-band beyond 15 km of the radar. In this icing case, the dynamics behind the cold front were sufficient to provide some lift and lead to production of cloud drops not detectable by CSU-CHILL at 30-km range. This fact alone would argue for the polarized NEXRAD IHL product to eventually be part of a system which includes other components more able to detect all scenarios of in-flight icing.

4.1.2 Comparison of IHLA results for icing and non-icing cases

On 30 December 2010 at 1906 UTC (case A) the vertically-pointing NIRSS radiometer ILW was quite low at 0.04 mm suggesting no aircraft icing threat. On 18 May 2011 at 1959 UTC (case B) ILW was 0.18 mm indicating the presence of SLW and a possible aircraft icing hazard above the NIRSS site. There was also a nearby pilot report of moderate icing within 20 min of this event. In this section, the IHLA fields using radar volumes corresponding closest in time to these radiometer measurements are compared for cases A and B.

Figure 18 shows the Plan Position Indicators (PPI) of measured reflectivity from CSU-CHILL for the both cases. For case A, the icing case, the radar was scanning a sector from 180^o to 330^o azimuth. For case B, the non-icing case, the cloud was relatively shallow and there is no melting layer as surface temperature was below 0^{o}C and no inversion was present. The PPI shown in Fig. 18A is at 1.5^o elevation angle and indicates no precipitation was falling to the ground in the vicinity of CSU-CHILL. Even though the surface temperature was above 0^{o}C on 18 May, the cloud base was above the freezing level and all of the radar echoes resided at temperatures < 0^{o}C. The PPI shown in Fig. 1B is at 8.4^o elevation angle and shows that reflectivity near the NIRSS site (indicated with the white circle) was higher for the icing case at the elevation angles shown.

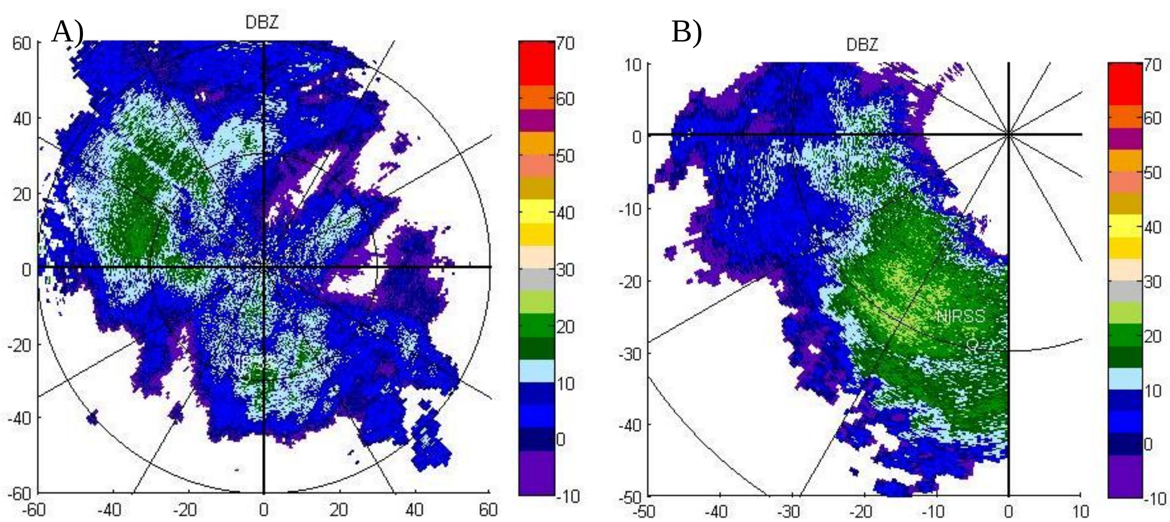

Figure 18: PPIs of measured reflectivity (dBZ), for A) non-icing case at 1.5^o elevation and B) icing case at 8.4^o elevation. The range rings are 30 km and the azimuth spokes are 30^o. The NIRSS site, located at 195^o azimuth and 30 km, is indicated by the white circle labeled NIRSS.

Next the feature fields of the NEXRAD Drizzle Detection Algorithm (MNDDA, or FRZDRZ in some figures) of the IHLA based on Ikeda et al. (2009) are compared for the two cases. The MNDDA output is a map in radar coordinates that ranges from 0 to 1 with 1 indicating the highest interest (or likelihood) for the presence of freezing drizzle.

The mean reflectivity feature field (MeanDBZ) is shown for the non-icing (A) and icing cases (B) in Fig. 19. The MNDDA's highest interest for freezing drizzle is between -10 and 5 dBZ. The MeanDBZ feature field > 5 dBZ above the NIRSS site at the elevation shown for both cases and thus is not indicating freezing drizzle for either case in that location. Figure 20 shows PPI plots of the local standard deviation of reflectivity (sdevDBZ). For the current sdevDBZ membership functions, the values with highest interest are $\leq$1 dB. Above the NIRSS site, sdevDBZ is >1 dB for both cases and thus does not indicate freezing drizzle. However there are lower values of sdevDBZ in the radar domain and near to the NIRSS site in both cases indicating an increased liklihood of freezing drizzle from sdevDBZ. Figure 21 shows PPI plots of the texture of reflectivity (TDBZ). Similar to sdevDBZ, the values of TDBZ with highest interest for freezing drizzle are low with the highest interest for 1 dB or below. In Fig. 21 the TDBZ is large and does not indicate freezing drizzle over NIRSS for either case. Once again there are lower values of TDBZ in the radar domain and near NIRSS in both cases indicating an increased likelihood of freezing drizzle being indicated by TDBZ.

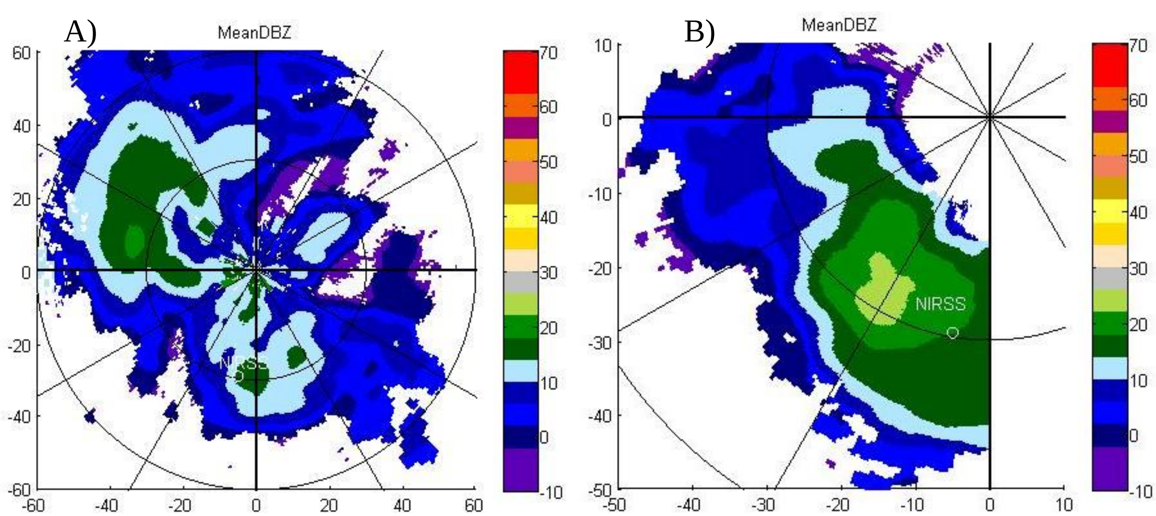

Figure 19: Same as Fig. 18 except the MNDDA feature field mean reflectivity (MeanDBZ) is shown.

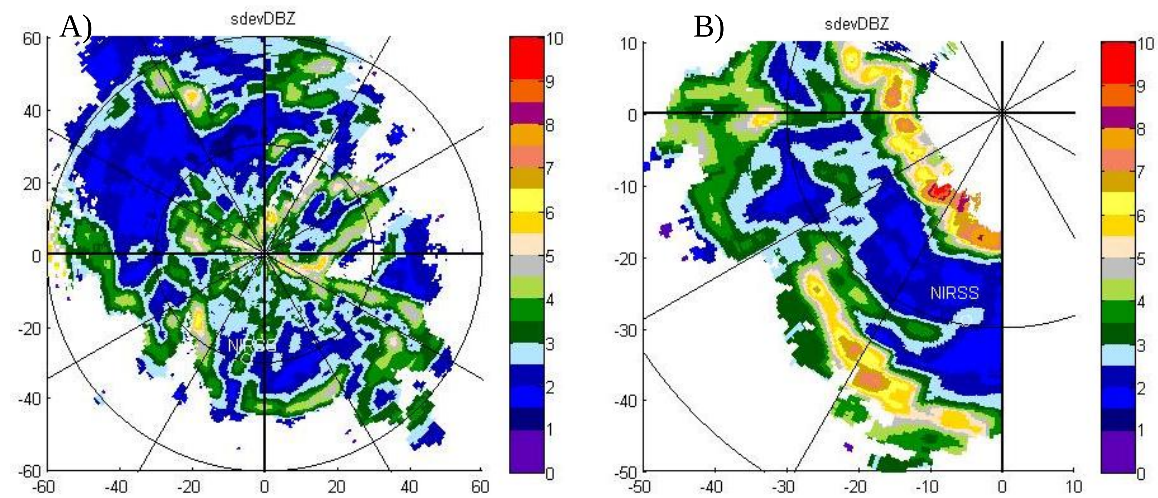

Figure 20: Same as Fig. 18 except the MNDDA feature field sdevDBZ is shown.

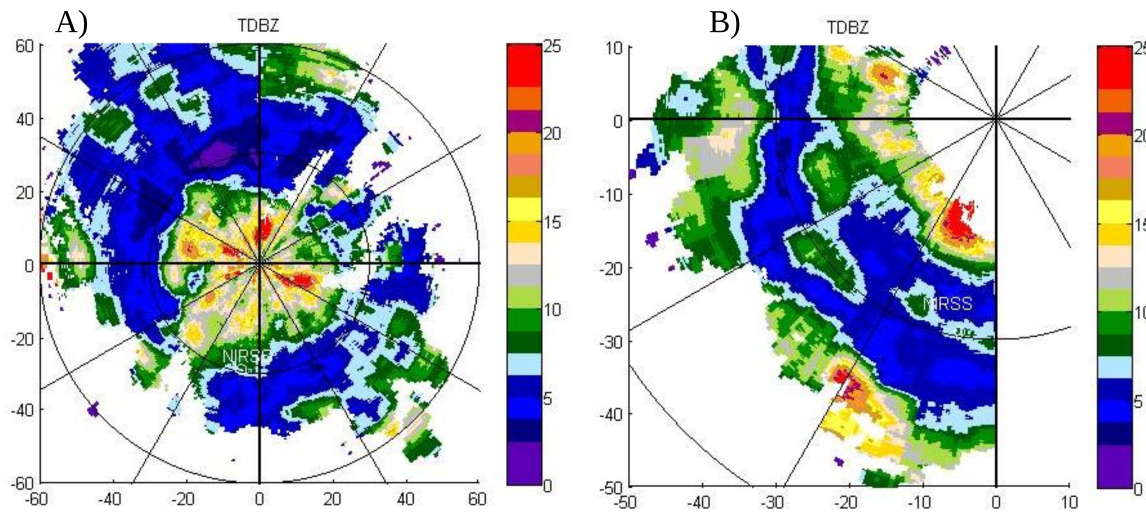

Figure 21: Same as Fig. 18 except the MNDDA feature field TDBZ is shown.

The vertical profiles over the NIRSS site of the feature fields illustrated in the PPI plots of Figs. 18 -- 21 are shown in Fig. 22 (the height is km above ground). Also plotted is the median of the reflectivity (MedDBZ) computed over the same area as the other feature fields. None of these feature fields strongly indicates freezing drizzle over the NIRSS site at either location with the exception of MeanDBZ at an altitude of 1.4 km for case B (Fig 5B).

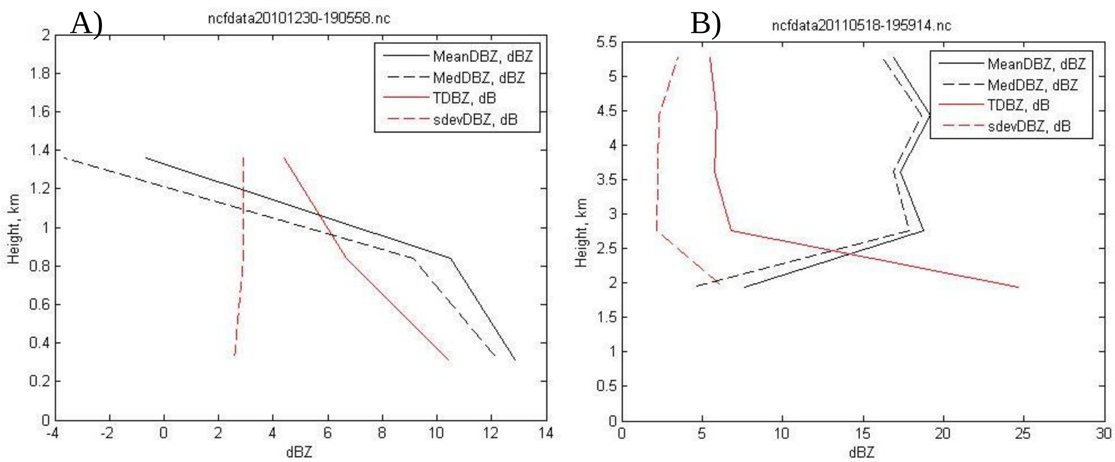

Figure 22: Vertical profiles of the MNDDA feature fields of MeanDBZ, TDBZ and sdevDBZ. The median reflectivity (MedDBZ) computed over the same spatial area is also shown. The non-icing case is shown in A) and the icing case is shown in B).

Figure 23 shows the PPI plots of the feature field of the median of the standard deviation computed over successive 15-km rings (med15_sdevDBZ). The highest interest for med15_sdevDBZ to indicate icing are values <3 with values as high as 4.5 indicating some degree of freezing drizzle signature from med15_sdevDBZ over the NIRSS site. Both days have freezing drizzle indicated by the med15_sdevDBZ feature field. The icing case has lower values of med15_sdevDBZ over NIRSS indicating a higher interest in freezing drizzle. Figure 24 shows a vertical profile of the med15_sdevDBZ feature field over the NIRSS site for both days. The values are all <4.5, thus this feature field shows at least some indication of freezing drizzle at most heights on both days.

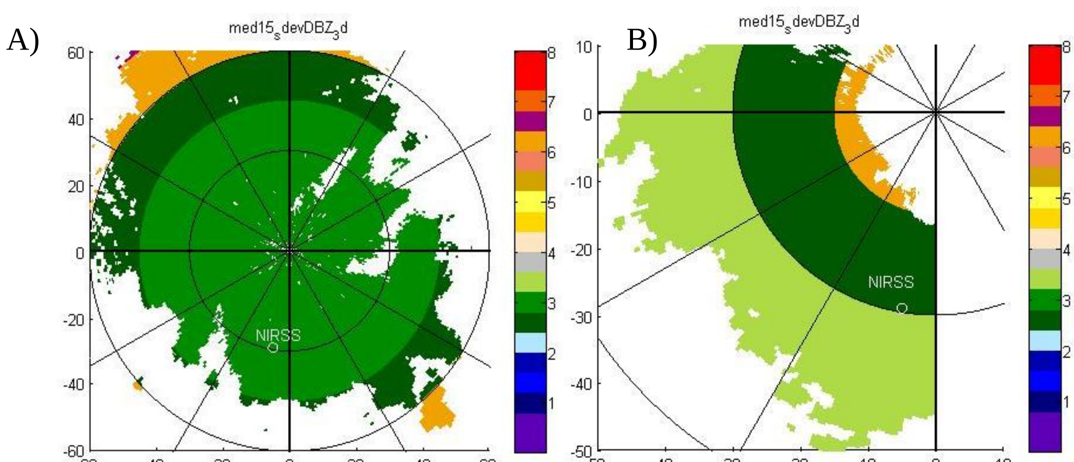

Figure 23: Same as Fig. 18 except for the MNDDA feature field median of the standard deviation computed over successive 15-km rings (med15_sdevDBZ) is shown.

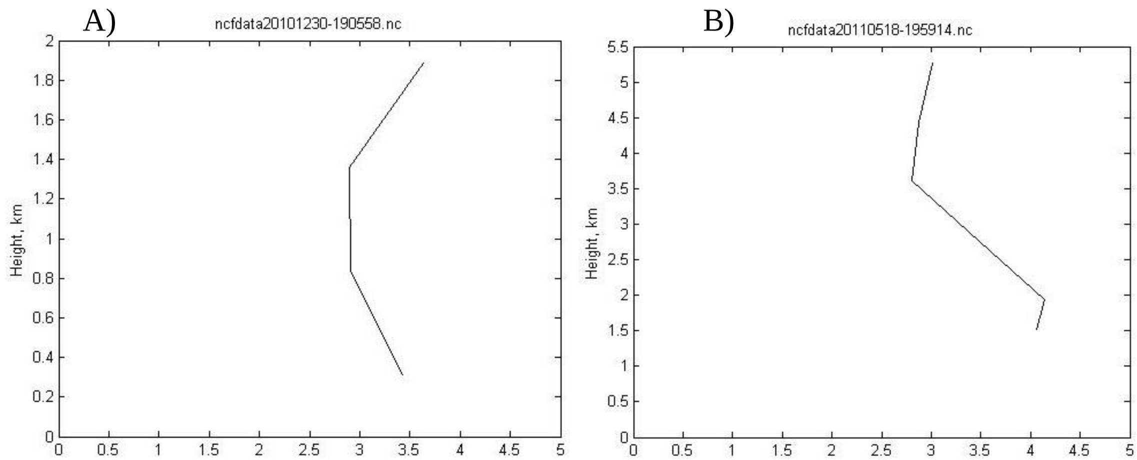

Figure 24: Same as Fig. 22 except the MNDDA feature field med15_sdevDBZ_3d is shown.

PPI plots of the MNDDA output field are shown in Fig. 25 for the non-icing and icing cases. At the elevation angle plotted, MNDDA indicates correctly that there is no freezing drizzle (Fig. 25A) over the NIRSS site in the non-icing case. The MNDDA output also does not indicate freezing drizzle near the NIRSS for the icing case. Figure 26 shows the vertical profile over NIRSS of the final MNDDA output field for both cases. There is only one indication of freezing drizzle over the NIRSS site, for the non-icing case at the highest altitude measured by CSU-CHILL. This was a false alarm. The fact that MNDDA does not indicate freezing drizzle above NIRSS for the icing case when significant ILW was measured is not necessarily a missed detection of icing conditions, it merely signifies that there was likely no freezing drizzle present.

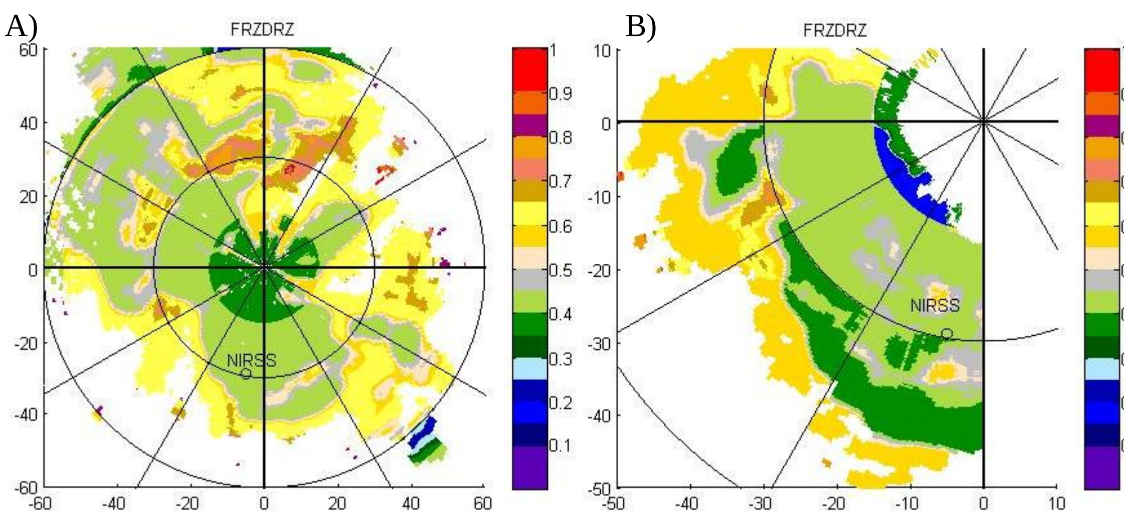

Figure 25: Same as Fig. 18 except the final MNDDA output is shown.

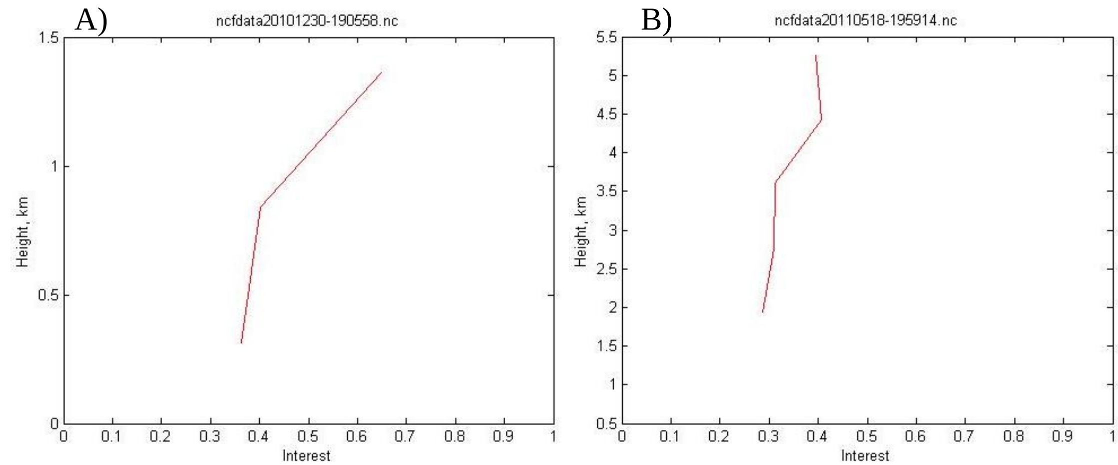

Figure 26: Same as Fig. 22 except the final MNDDA output is shown.

The SLWA utilizes feature fields derived from the dual-polarimetric variables Z_{dr} and K_{dp}. The SLWA output is a map in radar coordinates that ranges from 0 to 1 with 1 indicating the highest interest (or likelihood) for the presence of SLW. Plummer et al. (2010) characterized the dual-pol measurements using aircraft-radar comparisons taken during the MAP (Mesoscale Alpine Program) in northern Italy. They found icing conditions more likely to be present in regions with Z_{dr} and K_{dp} both near zero and with narrow distributions of values.

Figure 27 shows the PPI plots of measured differential reflectivity (Z_{dr}). The Z_{dr} on the non-icing case shows a wide range of values. There are very low Z_{dr} near the radar and quite high values, 1-3 dB, in layers beyond 30 km. In the icing case, the Z_{dr} values have values generally vary from 0.0 to just over 0.5 dB. The PPIs of the mean of Z_{dr} feature field (MeanZDR) computed over a local area are plotted in Fig. 28 for both cases. For the SLWA, MeanZDR values less than ~0.2 dB are more likely to contain liquid water than higher MeanZDR values. Near NIRSS the MeanZDR is quite low and indicates higher likelihood of SLW for the icing case. Meanwhile, for the non-icing case, the MeanZDR is higher and would not indicate SLW for the microphysical conditions considered in Plummer et al. (2010).

Figure 29 shows PPI plots of the standard deviation of Z_{dr} feature field (sdevZDR). The sdevZDR is lower near NIRSS for the icing case than for the non-icing case. For the SLWA, sdevZDR values less than ~0.2 indicate icing. For the icing case the sdevZDR feature field is low and indicates SLW near NIRSS and also in a nearby widespread region. The sdevZDR values for the non-icing case are much higher and do not indicate SLW.

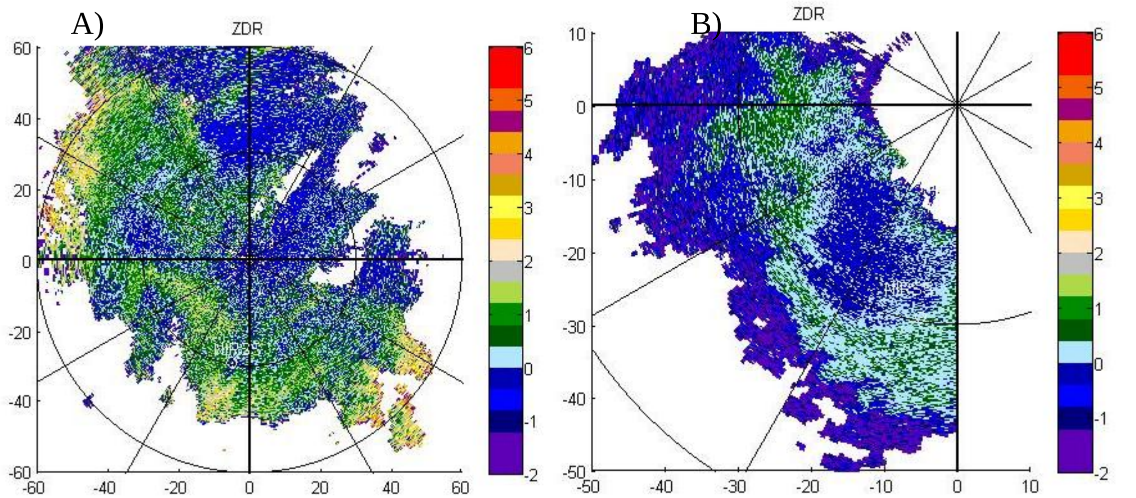

Figure 27: PPIs of measured differential reflectivity (Z_{dr}), for A) non-icing case, 1.5^o elevation, and B) icing case, 8.4^o elevation. The range rings are 30 km and the azimuth spokes are 30^o. The NIRSS site, located at 195^oazimuth and 30 km, is indicated by the white circle labeled NIRSS.

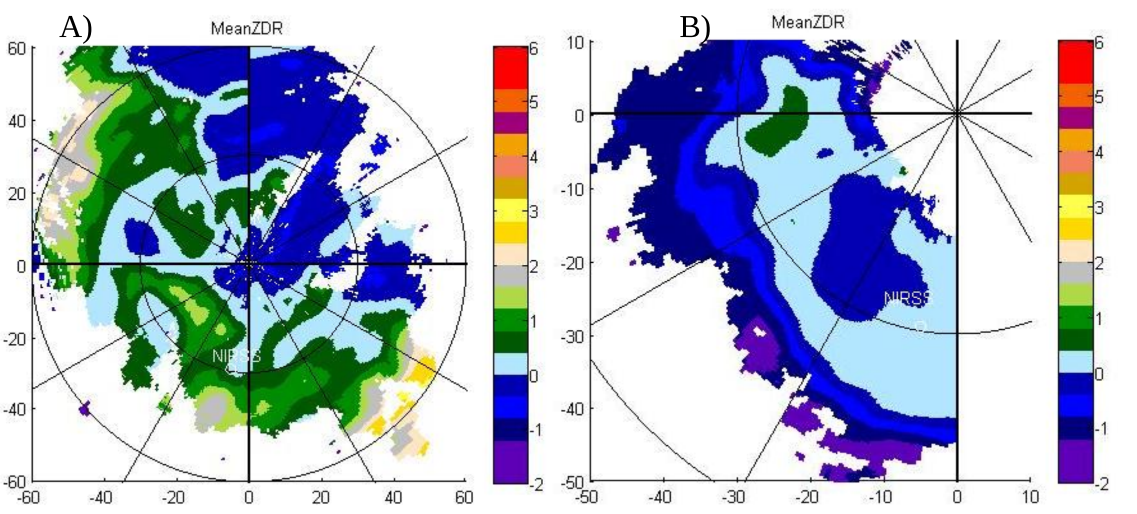

Figure 28: Same as Fig. 27 except the SLWA feature field MeanZDR is shown.

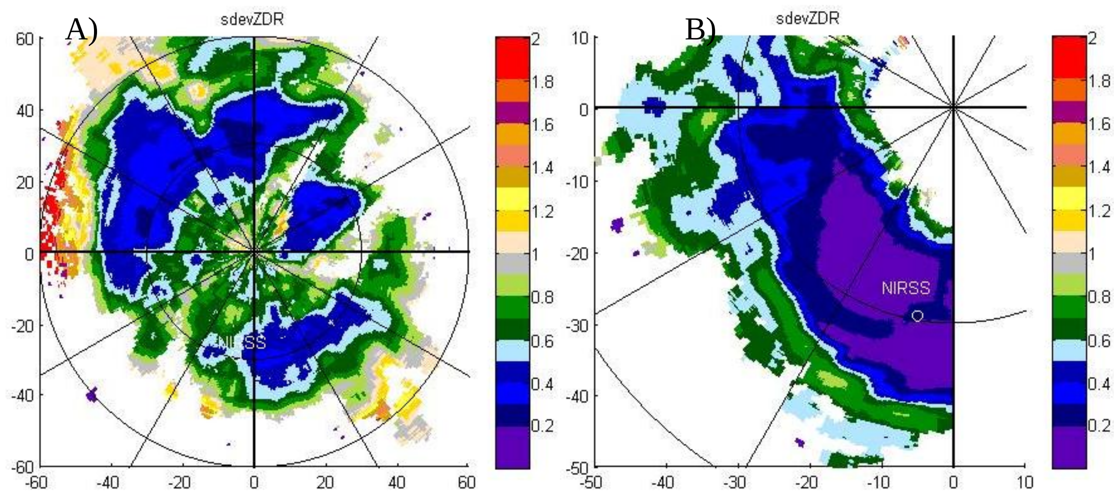

Figure 29: Same as Fig. 27 except the SLWA feature field sdevZDR is shown.

Figure 30 shows the vertical profiles of the Z_{dr} feature fields used in SLWA, MeanZDR and sdevZDR. Also shown are the median of Z_{dr} (MedZDR) and the texture of Z_{dr} (TZDR). It can be seen that over the NIRSS site, the MeanZDR values are >0.25 dB at all levels for the non-icing case indicating a low interest in SLW. At the same time the MeanZDR values are $\leq$0.2 dB for almost all levels in the icing case, indicating a high interest in SLW. Similarly the sdevZDR values are >0.5 for the no-icing case, indicating no interest in SLW. For the icing case the sdevZDR values are <0.25 (except the lowest level) indicating a high interest in SLW.

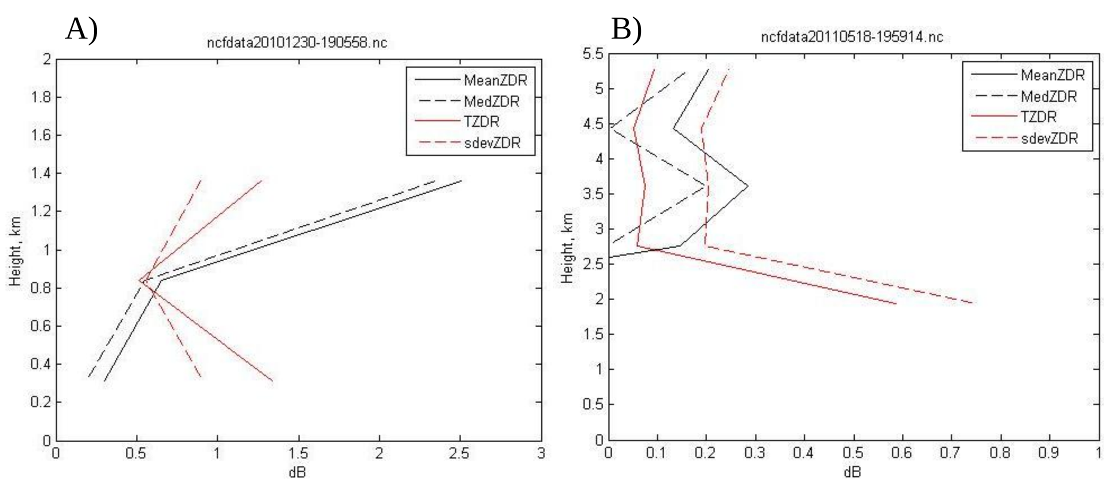

Figure 30: Vertical profiles of the SLWA feature fields MeanZDR and sdevZDR. The median Z_{dr} (MedZDR) and texture of Z_{dr} (TZDR) computed over the same spatial area are also shown. The non-icing case is shown in A) and the icing case is shown in B).

Figure 31 shows the PPI plots of measured specific differential phase (K_{dp}). The PPIs of the mean of K_{dp} feature field (MeanKDP) computed over a local area are plotted in Fig. 32 for the non-icing case (Fig. 32A) and the icing case (Fig. 32B). For the SLWA, the MeanKDP membership functions are set so that values less than about 0.1 dB are more likely to contain liquid water than higher MeanKDP values. Near NIRSS the MeanKDP is quite low and indicates higher likelihood of SLW for both icing and the non-icing cases. Figure 33 shows PPI plots of the standard deviation of K_{dp} feature field (sdevKDP). The sdevKDP is lower near NIRSS for the icing case than for the non-icing case (Fig. 33A). For the SLWA, sdevKDP values less than about 0.1 indicate icing. The sdevKDP values are similar for both cases near NIRSS.

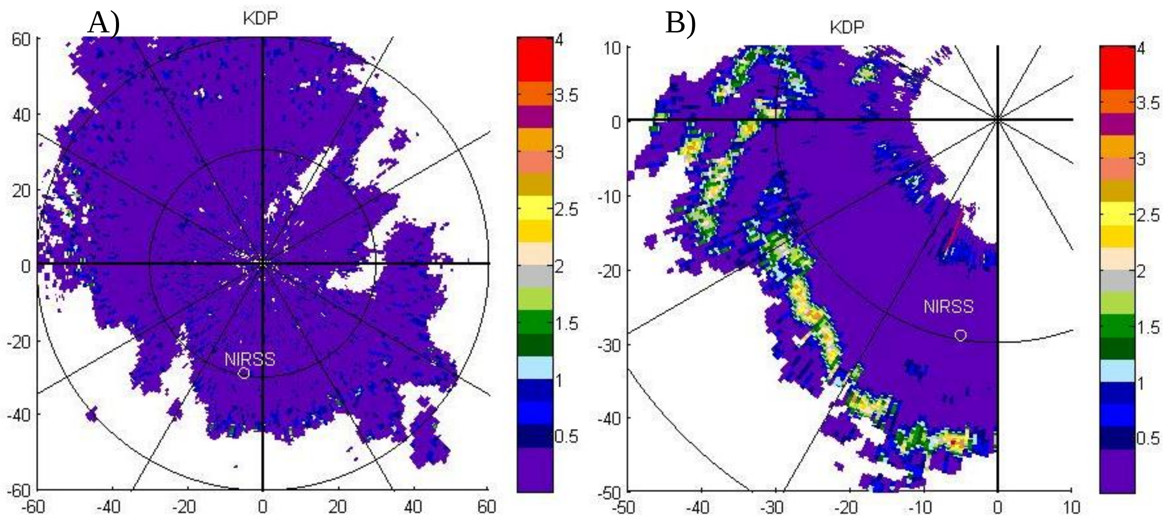

Figure 31 Same as Fig. 22 except the measured K_{DP} is shown.

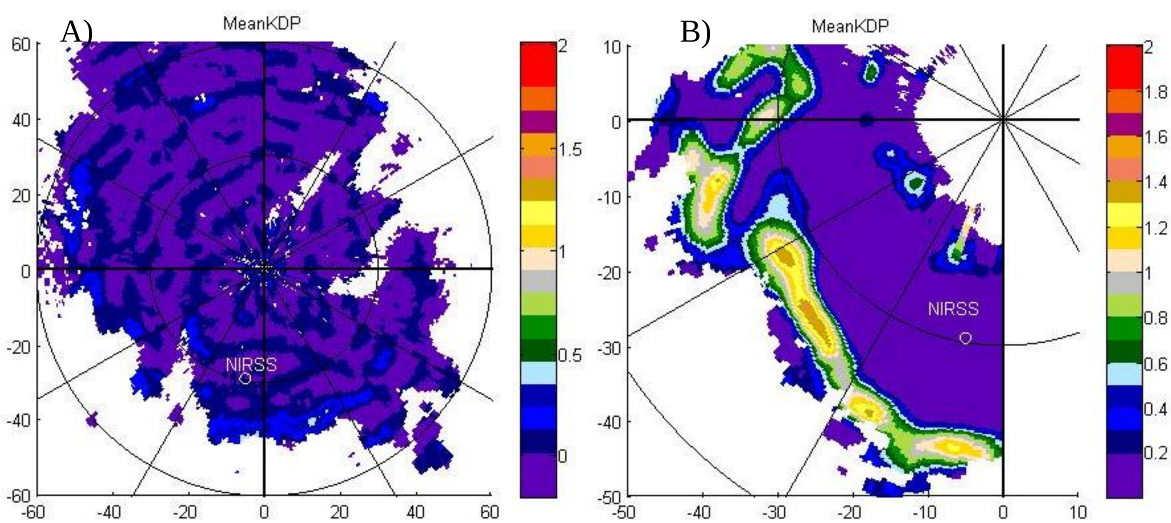

Figure 32: Same as Fig. 22 except the SLWA feature field of MeanKDP is shown.

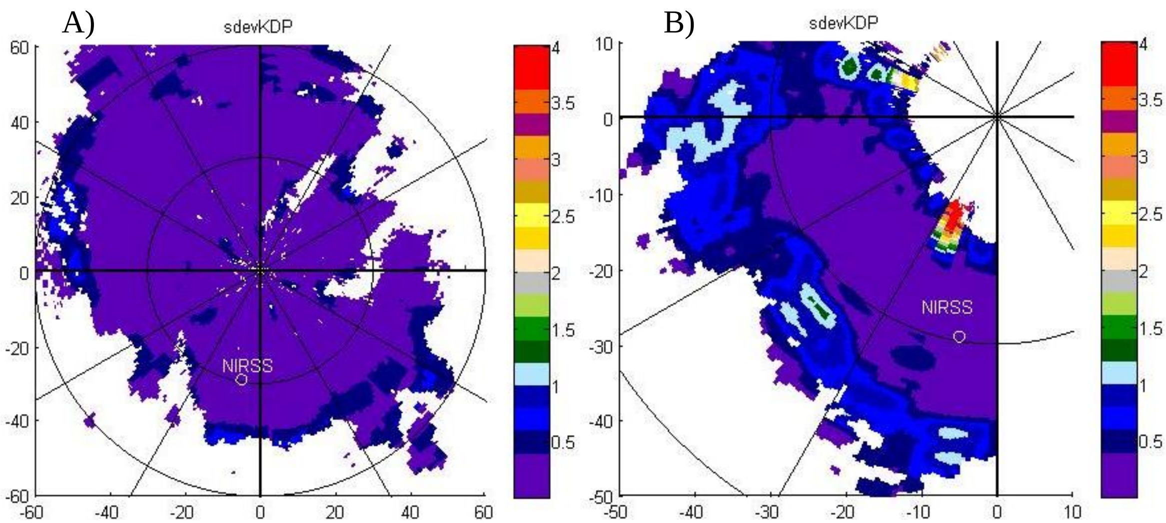

Figure 33. Same as Fig. 22 except the SLWA feature field of sdevKDP is shown.

Figure 34 shows the vertical profiles of the K_{dp} feature fields used in the SLWA, MeanKDP and sdevKDP. Also shown are the median of K_{dp} (MedKDP) and the texture of K_{dp} (TKDP). It can be seen that over the NIRSS site, the MeanKDP values are near zero at all levels for the both cases indicating a high interest in SLW. On the other hand the sdevKDP values are >0.2 over NIRSS for both cases indicating little to no interest in SLW.

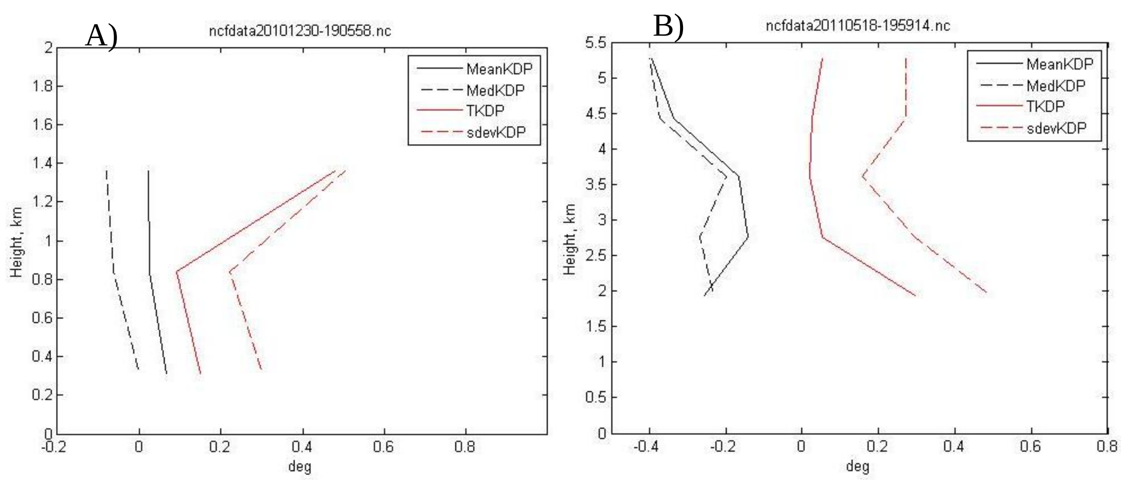

Figure 34: Same as Fig. 30 except the SLWA K_{dp} feature fields are shown.

The final SLWA output fields are plotted in Figure 35 for the non-icing and icing cases. At the elevation angles plotted, SLWA indicates correctly that there is no SLW (Fig. 35A) over the NIRSS site for the non-icing case. However, for the icing case the SLWA output shows a positive indication of icing with values >0.5 directly over the NIRSS site and a widespread region of higher values nearby.

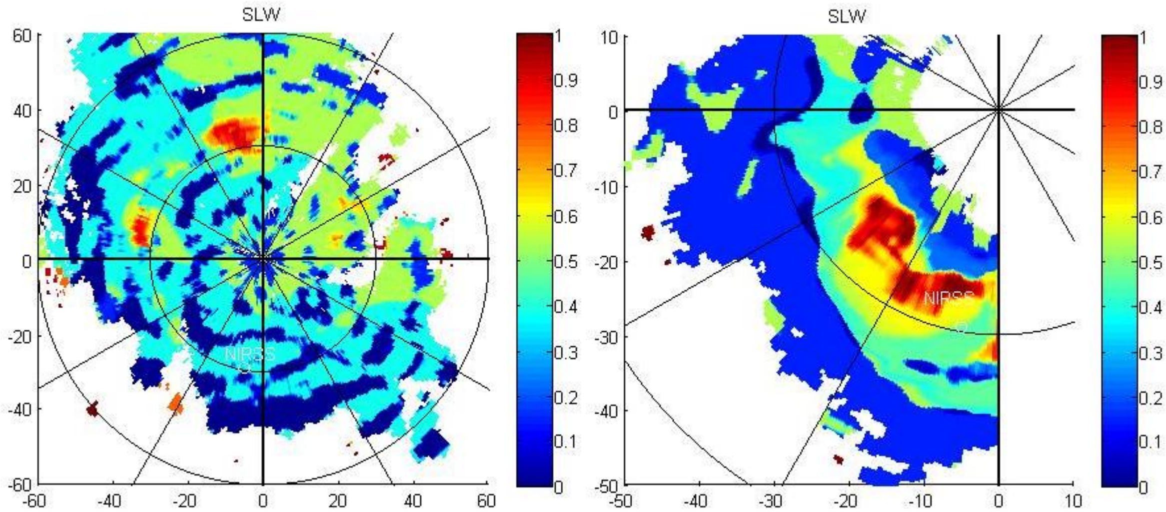

Figure 35: Same as Fig. 22 except the SLWA final output field is shown.

Figure 36 shows the vertical profile of the SLWA output field for both cases and reproduces the MNDDA output (from Fig. 26) for reference. For the non-icing case SLWA values are <0.4 for all altitudes indicating a low likelihood of icing due to the conditions for which the SLWA is tuned. For the icing case, the SLWA output shows increased values up to ~0.6 with all levels >0.5 except one. Thus there is a positive indication of icing conditions for the icing case with a lower likelihood indicated for the non-icing case.

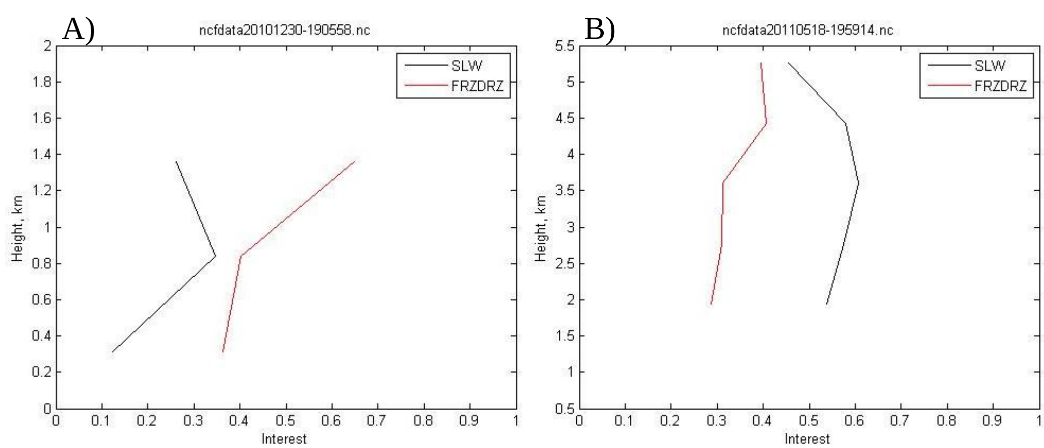

Figure 36: Vertical profiles of the final SLWA and MNDDA output fields for the icing (A) and non-icing (B) cases.

4.2 Discussion

Even though the NIRSS did not detect any ILW at 1900 UTC for the non-icing case, high values of ILW were measured at various times on 30 December, indicating transient icing conditions. The feature fields of the SLWA moved in the opposite direction than would be indicated by the SLWA membership functions. For example, the values of MeanZDR and sdev ZDR increased during times when icing conditions were observed by NIRSS even though high SLW was expected for low values of those fields. Figure 37 shows the vertical profile of the SLWA Z_{dr} feature fields for 30 December at 1729 UTC when the NIRSS radiometer-measured ILW was 0.13 mm, suggesting icing. Comparing with the non-icing case shown in Figure 34, there is an increase in the sdevZDR field at 1729 UTC and a layer of MeanZDR around 3.5 dB. A reasonable explanation for this apparent contradiction is that the icing conditions on 30 December resulted from a different microphysical process than the icing conditions studied by Plummer et al. (2010). The dual-polarimetric radar measurements on 30 December match well the mixed phase icing conditions described in Williams et al. (2011), with a layer of moderately high Z_{dr} and reflectivity values between 10 and 30 dBZ. In the next section an algorithm additional to MNDDA and SLWA is developed to identify the conditions described by Williams et al. (2011).

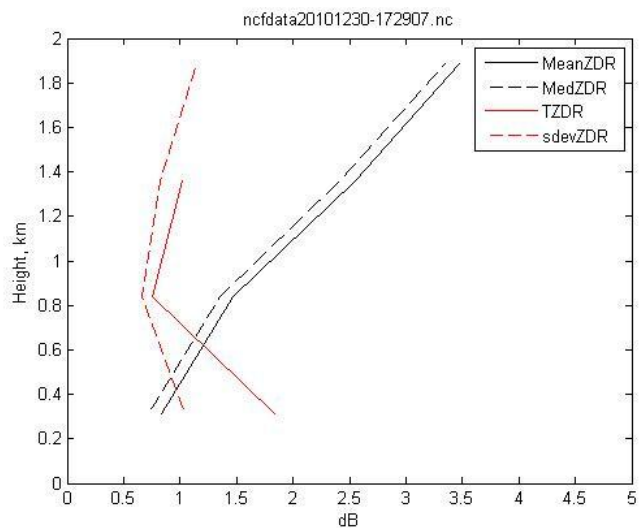

Figure 37. Vertical profiles of the SLWA feature fields MeanZDR and sdevZDR. The median Z_{dr} (MedZDR) and texture of Z_{dr} (TZDR) computed over the same spatial area are also shown. The data are from 30 December at 1729 UTC.

5. High Z_{dr} Algorithm

5.1 Introduction

Several recent studies shared the goal of determining the existence of icing conditions “indirectly” with polarimetric data by inferring the microphysical processes that produce SLW. The idea is that these microphysical processes may yield precipitation particles with polarimetric signatures that will indicate the existence of SLW. Many researchers are now investigating this. Williams et al.

(2011) describe the microphysical processes and includes a list of the relevant literature. The central idea is that different types of ice crystals form under the conditions of 1) ice saturation (no SLW) and 2) water saturation (SLW). Laboratory experiments and experimental measurements show that 1) supports pristine ice crystal growth such as plates and columns which have a relatively large fraction of ice to air. Under 2), dendrites grow, possibly with riming. The pristine type ice crystals that grow via vapor deposition are usually characterized by lower reflectivity values but can possess very high Z_{dr} values (>5 dB). The dendrites produced by the presence of SLW are typically less anisotropic, less dense (lower fraction of ice to air) but their growth is quite rapid and the ice particles are typically much larger than the ice particles due to 1). Very generally, the polarimetric signatures of 2) are higher reflectivity values than 1) and large Z_{dr} but lower than 1). The K_{dp} signatures of 1) and 2) overlap since K_{dp} is a function of the bulk density of the particles and their shape and orientation.

Experimental observations of 1) and 2) have been reported in the literature: Williams et al. (2011), Kennedy and Rutledge (2011), Ryzhkov et al. (2011), Bechini et al. (2011), Hogan et al. (2002). Recently, the S-PolKa radar facility was deployed at Addu Atoll in the Maldive islands, as part of the DYNAMO field experiment. Such high Z_{dr} measurements were seen frequently in the ice phase of storms, an example of which is given in Fig. 38 (reflectivity) and Fig. 39 (Z_{dr}). High Z_{dr} values are evident in the bright band, but large areas of higher Z_{dr} are evident in the ice phase also. Some of the highest Z_{dr} were on the western edge of the storm as indicated in orange on this color scale. The highest Z_{dr} were 8 to 9 dB. The reflectivities in this area ranged from -10 to 10 dBZ. Thus, these ice crystals are likely produced from Condition 1.

The continued existence of SLW for condition 2) is dependent, in part, on updraft strength (Williams, et al., 2011, Fig. 3). Updraft velocities are seldom available with sufficient precision (~cm s^{-1}), even if dual-Doppler capability were available. The NIRSS system can estimate vertical velocity from an analysis of the spectra from the vertically-pointing K_a-band radar and is discussed in one of the case studies included in this report. With the absence of the needed updraft to support the continued existence of SLW, the ice crystals begin to descend at a greater rate and the SLW is rapidly depleted due both to riming and preferred deposition. However, the types of ice crystals present will likely remain about the same, at least in short time periods, and the polarimetric signatures, which are dependent on these ice particles, will also likely remain about the same. Nevertheless, the existence of polarization signatures for 2) indicate that SLW is currently present or recently existed and thus is a good indication of possible SLW and icing conditions.

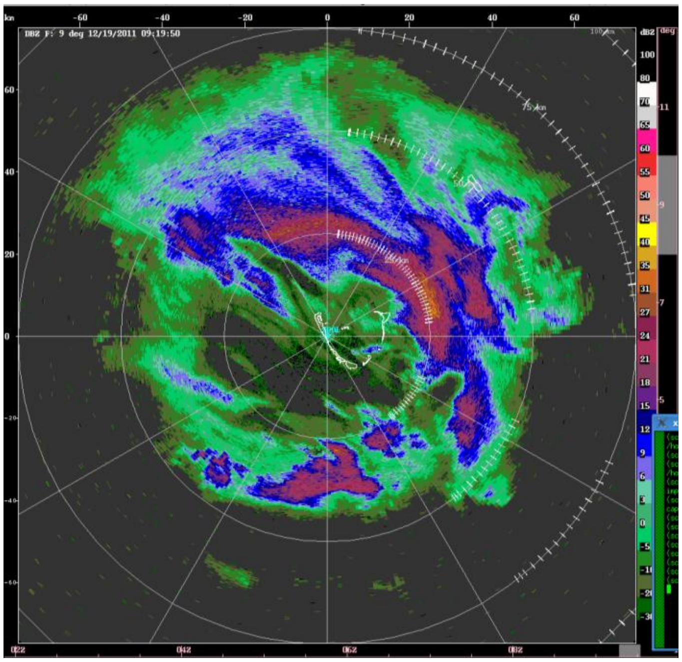

Figure 38 : Reflectivity from S-Pol data obtained on the Addu Atoll, Maldives at 12:19:50, 19 December, 2011 at an elevation angle of 9^o.

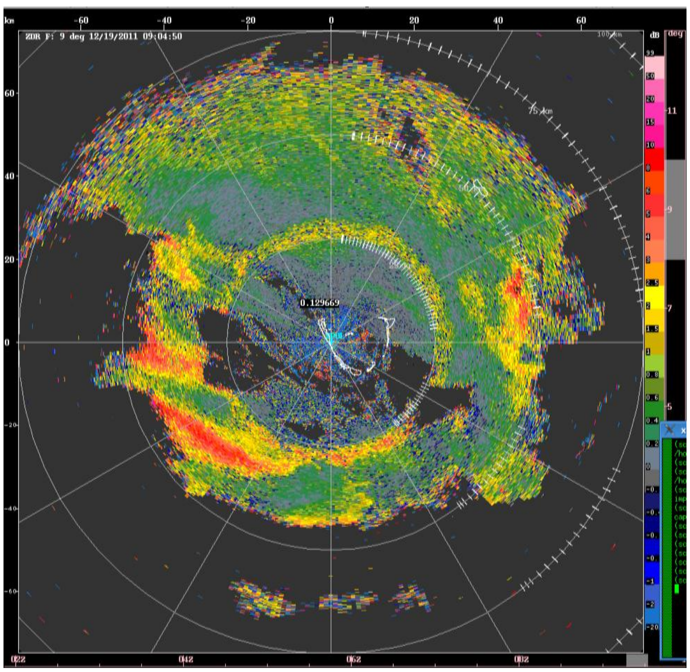

Figure 39: As for Figure 1, except that Z_{dr} is shown.

This category of icing polarimetric signatures was not considered in the FY10 IHL Final Report nor is it included in the IHLA algorithm delivered here as part of this report. However, next we describe and show results from a preliminary version of a new module that utilizes the icing category 1) described above. The module, dubbed the High Zdr Algorithm (HZDRA), utilizes the polarimetric signatures described in Williams et al. (2011). The full development, testing and inclusion of HZDRA into IHLA are left as future work.

5.2 Preliminary HZDRA

For the case of 30 December 2010, an elevated layer of Z_{dr} between 1 and 3 dB with reflectivity values of 10 - 30 dBZ became evident at 1730 UTC and persisted for about two hours. The NIRSS radiometer measured periods of high ILW as well as periods of insignificant ILW. The reflectivity and Z_{dr} values of icing case generally fit Category A defined by Williams et al. (2011, referred to here as "Category A") indicating mixed-phase conditions. Since these conditions can be transient for a number of reasons, it may not be surprising that the NIRSS system measured periods with both significant ILW and close to none.

At about 17:30 UTC the NIRSS radiometer measured an ILW of 0.12 mm and a PIREP was logged nearby at that time. Neither the SLWA nor the MNDDA identified potential icing conditions characterized by high Z_{dr} because they are tuned to detect different microphysical conditions with different radar signatures. In order to identify Category A conditions, a new module needs to be added to the IHLA. Figure 40 shows PPI plots of reflectivity and Z_{dr} for 30 December at 1729 UTC at an elevation angle of 0.5^o. There is a layer evident, although somewhat intermittent, of elevated Z_{dr} with reflectivity values near 10 dBZ between 30 and 60 km range from CSU-CHILL.

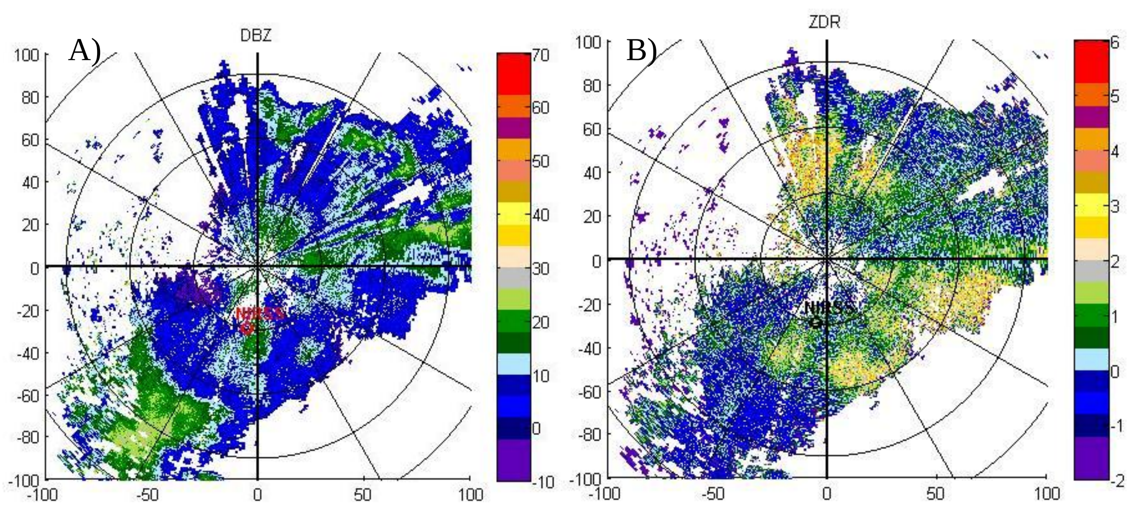

Figure 40: PPI plots of reflectivity A) and Z_{dr} B) from December 30th 2010 at 17:29 UTC. The NIRSS site is located at 195^o azimuth and 30 km range.

As a first step towards developing an algorithm to identify Category A conditions using layers of high Z_{dr}, a metric was defined based on the reflectivity and Z_{dr} values described in Table 1 of Williams et al. (2011). We call this the High Z_{dr}

algorithm, or HZDRA. This preliminary HZDRA utilizes the feature fields MeanDBZ and MeanZDR described in Section 4.2 for SLWA. The membership functions for icing conditions are shown in Fig.41. The MeanDBZ and MeanZDR feature fields are mapped into interest fields (int_MeanDBZ and int_MeaZDR) ranging from 0 to 1 using these membership functions.

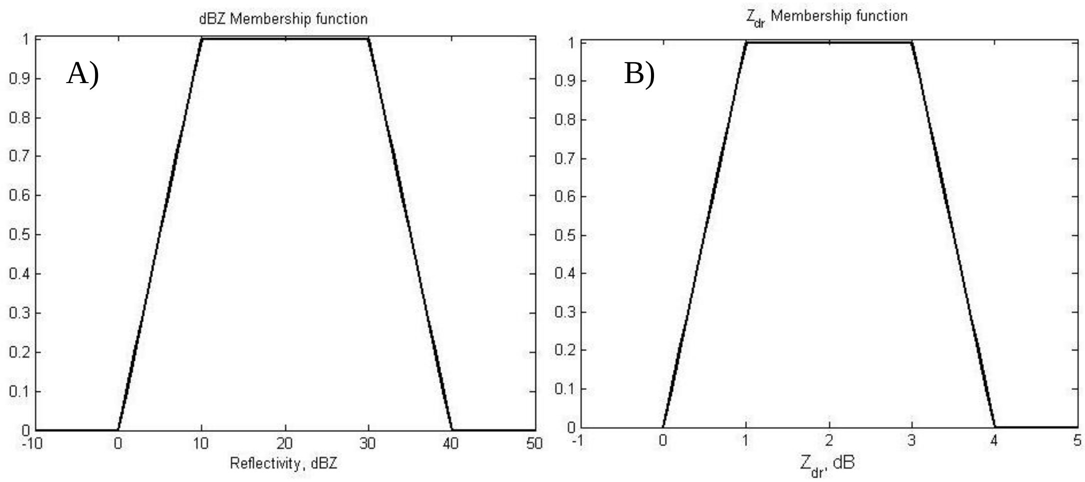

Figure 41: Membership functions for the HZDRA of reflectivity A) and Z_{dr} B).

Since the icing conditions HZDRA is trying to identify require *both* the reflectivity and Z_{dr} values to be within ranges specified by Williams et al. (2011), the combination of the two feature fields should accomplish an AND operation. Therefore to aggregate the int_MeanDBZ and int_MeanZDR interest fields we use a product, i.e., int_MeanDBZ * int_MeanZDR. The result is a final output ranging from 0 to 1, with 1 indicating the strongest likelihood of Category A icing and 0 indicating the weakest.

The advantage of using the product to aggregate the interest fields can be illustrated by a hypothetical example. Consider the case of reflectivity being equal to 15 dBZ and Z_{dr} being equal to 0 dB. In this case there is no evidence of Category A icing. The interest field of int_MeanDBZ will be 1 and int_MeanZDR will be 0. A weighted sum aggregation would result in a final result of 0.5, with equal weights on int_MeanDBZ and int_MeanZDR, which indicates some risk of icing. However the product would be 0, correctly indicating no risk of category A icing. However if the Z_{dr} values were 2 dB, with the same dBZ value, the product of the interest fields would correctly indicate 1.

5.3 HZDRA Results

Figure 42 shows the output of the HZDRA for the 30 December case at 1729 UTC at 0.5^o elevation angle (same as shown in Figure 42). The output identifies an icing risk associated with the layer of high Z_{dr} and reflectivity around 10 dBZ in a ring between 30- and 60-km range. The icing likelihood is high over the NIRSS site, where ILW values were around 0.13 mm.

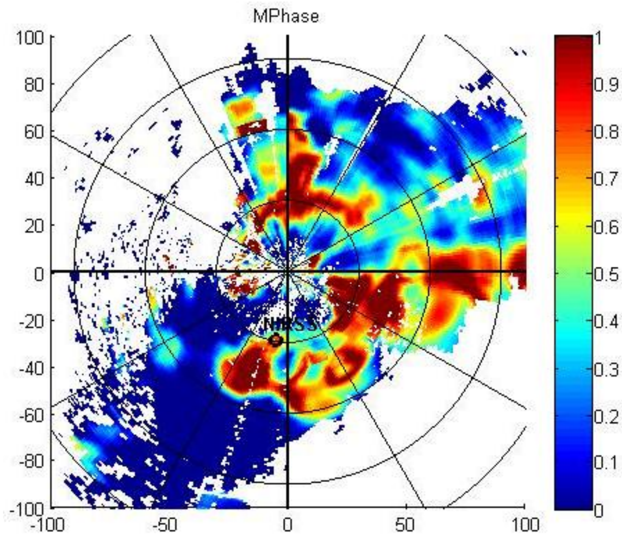

Figure 42: 0.5^o elevation PPI of the output of the preliminary HZDRA on 30 December at 1729 UTC.

The HZDRA was also run on the 18 May 2011 icing case and the results are shown in Fig. 43. In this case, a Category A icing threat was not detected, with HZDRA values below ~0.4 near the NIRSS site, despite the high ILW measured there. This is not a missed detection because the situation is not what the HZDRA is tuned for; recall that the SLWA *did* indicate icing in this case. This illustrates the strength of the modular design of the IHLA algorithm.

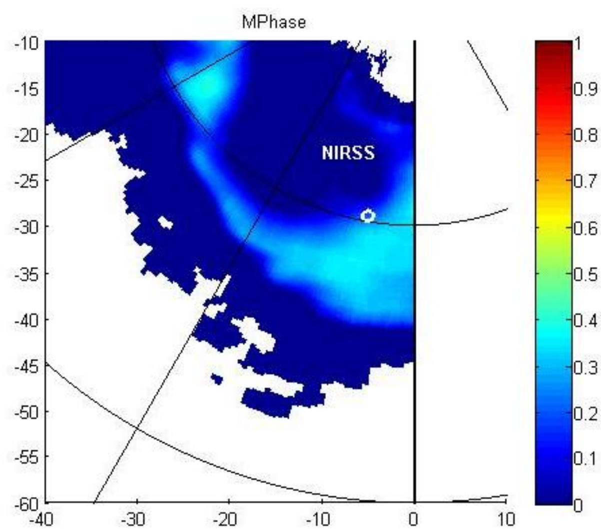

Figure 43: 0.5^o elevation PPI of the output of the preliminary HZDRA on 18 May at 1959 UTC.

Consider that the radar signatures identified by HZDRA may not coincide in space and/or time directly with the icing threat. The ice crystals responsible for the radar signature may be advected away or persist longer than the liquid water. However, these conditions can be readily identified and used to indicate an increased likelihood of icing threat in the area. Therefore we consider it important to include IHLA capability to identify these conditions.

The HZDRA, and results presented here, are encouraging but very preliminary. HZDRA needs to be further tested and tuned before it is incorporated into the IHLA. For example, there are numerous AND operators to choose from to aggregate the interest fields. Adding a temperature feature field to the algorithm can add skill. Other feature fields should be investigated in the context of the HZDRA, such as sdevZDR, MeanKDP, sdevKDP and others. Finally, the ring-finding algorithm used to find the bright band in FZLA could be modified to help identify the layers of high Z_{dr} associated with icing.

6. Summary

The icing hazard level algorithm was developed and delivered to MIT-LL per the contract obligations. Data gathered during a cooperative field program were used to improve the icing hazard level algorithm from the original, preliminary version written in the first part of this work completed in 2010. The effort put into the field program, including a subcontract to Colorado State University for radar data, was well worth it and produced a valuable data set for algorithm development. Additionally, a substantial portion of the work this year involved combining the code into a single end-to-end algorithm and the documentation of that algorithm.

The algorithm is based on published scientific research using S-band radars. It was tested on data from a research radar and validated using an remote sensor-based icing detection system designed by NASA, and by nearby pilot reports of icing conditions. Results to date look promising. Most of the freezing drizzle and supercooled liquid water algorithm fields are consistent with the presence or lack of icing conditions studied. There are, however, some exceptions and some of these are related to the limitations imposed by the algorithms used. The two main components, after all, were specifically designed for discrimination of freezing drizzle, ice crystal, and mixed-phase conditions which do not span all icing environments. As part of our effort for this contract we developed a new module for the IHLA termed the high Z_{dr} algorithm as reported in section 4.3. It is based on reports of icing in high Z_{dr} regions and on known microphysics that produce such polarimetric signatures. Suggestions for incorporating new techniques and other improvements are presented in the next section.

7. Future Work

Additional capabilities that could increase the versatility and skill of the IHLA are summarized below.

- Improvements:
  - Redesign the freezing level routine so that the freezing level becomes a function of azimuth angle. An azimuth angle increment of 30^o may be fine enough to capture the relevant freezing level variability of the environment.
  - Integrate the PID algorithm into the freezing level algorithm to help better define the variability of the freezing level.
  - The freezing level algorithm can effectively identify bands of elevated Z_{dr} that are indicative of icing hazard. This ability can be added to the elevated Z_{dr} icing detection routine.
  - The freezing level algorithm along with the PID can be used to identify multiple freezing levels. Output from the NWP model may also be used. Data cases are needed that exhibit the multiple freezing level polarimetric signatures.
  - Test and implement gridded temperature and humidity feature fields into fuzzy logic IHL, although it still needs to be demonstrated that incorporation of a full domain of gridded NWP model temperature is needed as opposed to one value over the whole grid.
  - Modify MNDDA algorithm to have elevation angle-dependent range resolution.
  - Incorporate more inference of microphysical conditions via polarization variables as discussed in Appendix A.
  - Implement a "high Z_{dr}" icing detection capability as discussed in Section 4.
  - Test the dependence of the feature fields with various operating configurations of the WSR-88D radars. The measurement variance of the radar data depends on the number of samples used, the scan rate, etc. Thus it is recommended to investigate the feature fields utilizing the local spatial standard deviation of radar measurements for the various Volume Coverage Patterns (VCPs). It may be necessary to define separate membership functions for different VCPs.
- Testing:
  - S-PolKa will be operational at its new site, called Firestone (just west of Firestone, CO, close to the NOAA Platteville field site) in September, 2012. The simultaneous S- and K_a-band radar data can help determine the existence of SLW. In fact, the SPolKa K_a-band radar was originally developed for aircraft icing detection. Thus additional data sets with independent verification of icing conditions could be gathered.

- Other applications:
    - Investigate the possibility of combining the IHLA with CIP.
    - Consider the output of the IHLA as a component of the new FAA program TAIWIS – Terminal Area Icing Weather Information System – which will develop improved detection and forecasting of freezing precipitation in the airport terminal area.

Acknowledgment

Both the CSU-CHILL and NCAR S-Pol radars are supported by the National Science Foundation. Any opinions, findings and conclusions or recommendations expressed in this publication are those of the authors and do not necessarily reflect the views of the National Science Foundation.

References

Bechini, R., R. Cremonini, L. Baldini, E. Gorgucci, and V. Chandrasekar, 2011: Observations of KDP in the ice region of precipitating clouds at X-band and C-band radar frequencies. . AMS 35th Conf. on Radar Meteorology, Pittsburgh, PA, 26-30 September. Available online.

Bernstein, B.C., F. McDonough, M.K. Politovich, B.G. Brown, T.P. Ratvasky, D.R. Miller, C.A. Wolff and G. Cunning, 2005: Current Icing Potential: Algorithm Description and Comparison with Aircraft Observations. *J. Appl. Meteor.*, **44**, 969-986.

Brunkow, D., Bringi, V. N., Kennedy, P, Rutledge, S., Chandrasekar, V., Mueller, E. and Bowie, R., “A description of the CSU–CHILL National Radar Facility”, *J. Atmos. Ocean. Tech*, **17**, Issue 12, pp. 1596-1608, 2000. Hogg, D.C., F.O. Guiraud, J.B. Snider, M.T. Decker and E.R. Westwater, 1983: A steerable dual-channel microwave radiometer for measurements of water vapor and liquid water in the troposphere. *J. Climate Appl. Meteor*., **22**, 789-806.

Ellis, S.M., D.Serke, J. Hubbert, D. Albo, A. Weekley and M.K. Politovich, 2011: In-flight icing detectin using S-band dual-polarimetric weather radar data. AMS 35th Conf. on Radar Meteorology, Pittsburgh, PA, 26-30 September. Available online.

Hogan, R., P. Field, A. Illingworth, R. Cotton, and T. Choularton, 2002: Properties of embedded convection in warm-frontal mixed-phase cloud from aircraft and polarimetric radar. *Quart. J. Roy. Met. Soc*., **128**, 451-476.

Ikeda, K., Rasmussen, R., Brandes, E. and McDonough,F., 2008: Freezing drizzle detection with WSR-88D radars”, *J.Appl. Meteor. Climatol*, **48**, 41-60.

Johnston, C.J., D. J. Serke, K. L. Elmore, A. L. Reehorst, and M. K. Politovich, 2012: Comparison of K_a-Band and Polarized S-Band Moment Profiles for Inference on Mixed-Phase Conditions. Presented at AMS 11th Student Conference and Career Fair, 22 Jan., New Orleans, LA.

Kennedy, P.C. and S.A. Rutledge, 2011: S-Band Dual-Polarization Radar Observations of Winter Storms. J. Appl. Meteor. and Clim., **50**, pp. 844 – 858.

Lakshmanan, V., K.L. Elmore, and M.B. Richman, 2010: Reaching Scientific Consensus Through a Competition. *Bull. Amer. Meteorol. Soc*., **91**, 1423-1427.

Plummer, D.M., S. Goeke, R.M. Rauber and L.DiGirolamo, 2010: Discrimination of mixed-versus ice-phase clouds using dual-polarization radar with application to detection of aircraft icing regions. *J. Appl. Meteor. Clim*., **49**, 920 – 935.

Reehorst, A.L., Brinker, D.J., Ratvasky, T.P., “NASA Icing Remote Sensing System: comparisons from AIRS–II,” NASA/TM—2005-213592, 2005.

Reehorst, A., Politovich, M., Zednik, S., Isaac, G. and Cober, S., “Progress in the development of practical remote detection of icing conditions”, *NASA/TM 2006-214242*, NASA, 2006.

Reehorst, A., Politovich, M. K., Zednik, S., Isaac, G. A., & Cober, S., Progress in the Development of Practical Remote Detection of Icing Conditions (NASA/TM 2006-214242). NASA, 2006.

Ryzhkov, A., H. D. Reeves, T. J. Schuur, M. R. Kumjian, and D. S. Zrnic, 2011: Investigations of polarimetric radar signatures in winter storms and their relation to aircraft icing and freezing rain. AMS 35th Conf. on Radar Meteorology, Pittsburgh, PA, 26-30 September. Available online.

Serke, D. J., F. McDonough and M. Politovich, 2008: Analysis of 3-D NEXRAD Mosaic reflectivity data collocated with research aircraft and satellite data: implications on in-flight icing”. 13th Conference on Aviation, Range and Aerospace Meteorology, New Orleans, LA, Jan 20-25. Available online.

Serke, D.J., J., Hubbert, S. Ellis, A. Reehorst, P. Kennedy, D. Albo, A. Weekley and M. Politovich, 2011: The winter 2010 FRONT/NIRSS in-flight icing detection field campaign. AMS 35th Conf. on Radar Meteorology, Pittsburgh, PA, 26-30 September. Available online.

Solheim, F., Godwin, J., Westwater, E., Han, Y., Keihm, S., Marsh, K., and Ware, R., “Radiometric profiling of temperature, water vapor and cloud liquid water using various inversion methods”, *Radio Science*, **33**, 393-404, 1998.

Vivekanandan, J., S.M. Ellis, R. Oye, D. S. Zrnic, A. V. Ryzhkov and J. Straka, 1999: Cloud Microphysics Retrieval Using S-band Dual-Polarization Radar Measurements. *Bull. Amer. Meteor. Soc*., **80**, 381-388.

Williams, E.R., D. J. Smalley, M. F. Donovan, R. G. Hallowell, K. T. Hood, B. J. Bennett, R. Evaristo, A. Stepanek, T. Bals-Elsholz, J. Cobb, and J. M. Ritzman, 2011: Dual polarization radar winter storm studies supporting development of NEXRAD-based aviation hazard products. AMS 35th Conf. on Radar Meteorology, Pittsburgh, PA, 26-30 September.

Appendix A: Glossary

AGL	(height) Above Ground Level
CIP	Current Icing Product
CMD	Clutter Mitigation Decision
CSU-CHILL	Colorado State University – University of Chicago – Illinois State Water Survey S-band polarized research radar
FAA	Federal Aviation Administration
FIP	Forecast Icing Product
GMAP	Gaussian Model Adaptive Processing
GRC	(NASA) Glenn Research Center
IHL	Icing Hazard Level
IHLA	Icing Hazard Level Algorithm
ILW	Integrated Liquid Water
IWV	Integrate Water Vapor
K_{dp}	Radar specific differential phase
MNDDA	Modified NEXRAD Drizzle Detection Algorithm
MSL	(height above) Mean Sea Level
NASA	National Aeronautics and Space Administration
NCAR	National Center for Atmospheric Research
NDDA	NEXRAD Drizzle Detection Algorithm
NEXRAD	Next Generation Radar
NIRSS	NASA Icing Remote Sensing System
NOAA	National Oceanic and Atmospheric Administration
NWP	Numerical Weather Prediction
NSF	National Science Foundation
NWS	National Weather Service
ORPG	(NEXRAD) Open Radar Products Generator
PIREP	(voice) Pilot REPort
PPI	Plan Position Indicator (radar scan display)
RUC	Rapid Update Cycle (NWP model)
SLW	Supercooled Liquid Water
SPolKa	(NSF's) S-band Polarized radar with added K_a-band capability
WRF-RAP	Weather and Research Rapid Refresh (NWP model)
Z_{dr}	Radar differential reflectivity
ρ_{hv}	Radar correlation coefficient

Appendix B: Case Study Meteorological Descriptions

7 December 2010

Significant Weather Features

Surface/Meteogram

0000 UTC to 0600 UTC

At 07/0000 UTC a trough was formed along the Front Range Mountains of CO. The low that was associated with this trough was over South/Central CO. A small area of clouds stretched from Northeast CO into WY. The CTT over the Front Range communities was near -25 °C to -30 °C. By 07/0300 UTC a new low formed over Denver which was not a strong low only 1020 mb in MSLP. The same low was still over South/Central CO and also was not strong at 1020 mb in MSLP. The CTT over the Front Range communities was near -5 to -10 °C. At KDEN the temperature dropped from 41 to 36 °F. Visibility was between 9 and 10 mi. Winds were variable around 5 kt over the time period. Cloud base heights were between 8500 and 14000 ft AGL. Pressure decreased from 1020 to 1018 mb over the time period.

0600 UTC to 1200 UTC

At 07/0600 UTC the trough was labeled a stationary front and had propagated slightly eastward over the High Plains of eastern CO. Two lows interconnected the stationary front. One low was over extreme Southeastern WY and the other low was over extreme Southeastern CO. There was varying amounts of stratocumulus clouds over Northeastern CO. The CTT near KDEN was at -25 °C. By 07/0900 UTC an open wave cyclone had formed over the NE Panhandle. The warm front was over extreme Eastern CO. Significant cloud cover was over Denver at this time. The CTT over KDEN was -35 °C to -40 °C. At KDEN the temperature dropped from 36 °F to 33 °F. Visibility was between 8 and 10 mi over the time period. Winds were variable from 07/0600 to 07/0800 UTC. After 07/0800 UTC winds were from the southwest between 5 and 10 kt. Cloud base heights were between 8500 and 14000 ft AGL. Pressure dropped slightly and climbed back to 1018 mb over the time period.

1200 UTC to 1800 UTC

At 07/1200 UTC the open wave cyclone had connected with the stationary front in extreme Northeastern NM. The low was still over the NE Panhandle. A band of clouds was over much of Eastern CO. The CTT over KDEN were between -5 °C and -10 °C. By 07/1500 UTC colder cloud tops had moved over KDEN. The warm front of the open wave had now become a stationary front. Over KDEN the CTT was near -20 °C. At KDEN the temperature increased from 33 °F to 42 °F. Visibility was at 10 mi. Winds were variable between from the northwest to the northeast over the time period. Cloud base heights were between 5000 and 14000 ft AGL. Pressure rose from 1018 mb to 1022 mb over the time period.

1800 UTC to 2400 UTC

At 07/1800 UTC the area of low pressure over the NE Panhandle had disappeared. A small inverted trough extended from Northeast CO through Central/South SD. A band of colder topped clouds were over Northeast CO at this time. The CTT over KDEN was near -15 °C. By 07/2100 UTC another small inverted trough developed across Northern CO into Southeastern WY. By this time there were no clouds over KDEN.

Upper Air

At 07/0000 UTC at 250 mb a small ridge was over the Central Plains region. A small trough was embedded in the flow over the Intermountain West region. At 500 mb the small trough becomes more noticeable over the Intermountain West region. In addition the ridge over CO did not look as strong as it was at 250 mb. At 700 mb a small lee-side trough was forming east of the Rocky Mountains in CO. This trough looked to be associated with a trough over the Northern and Central Rockies.

At 07/1200 UTC at 250 mb a small positively $_{\text{tilt}}$ed trough extended from Northeast CO into SD. A large ridge was propagating across the Intermountain West region at this time. At 500 mb the positively tilted trough was over much of CO and extended into SD. The -24 °C isotherm was over Central CO. At 700 mb an inverted trough was located over Southeastern CO and a portion of Western KS. In addition another small trough was over Southeastern WY.

Soundings

07/0000 UTC KDNR sounding: an inversion was in place from the surface to 800 mb. The sounding was dry from the surface to ~ 625 mb. The freezing level was at 700 mb. Above 625 mb to almost 400 mb there was a saturated layer. A very large inversion was positioned from 380 to 325 mb. This sounding only recorded winds from 220 mb and aloft

07/1200 UTC KDNR sounding: an inversion was in place from the surface to 810 mb. From the surface to 380 mb the sounding was dry. Winds veered from the surface to 650 mb. Winds at the surface were from the southwest at 5 kt. At 650 mb the winds were from the northwest at 25 kt. Above 650 mb winds remained from the west/northwest.

Best Icing Time Periods: 07/1320 UTC through 07/0240 UTC

Data Availability

PIREPs: 3 PIREPs within a 30-km radius of Platteville site.
CHILL: Initiates: 07/1642 UTC
PPIs: 07/1642 UTC through 07/1748 UTC.
NIRSS: All NIRSS data are present.

30 December 2010

Significant Weather Features

Surface/Meteogram

0000 UTC to 0600 UTC

At 30/0000 UTC two lows were near and over CO. One low was over NW NE/SW SD and the other low was over extreme SE CO. Both lows had troughs that extended southwest from the central part of the low. The low over SE CO created an upslope pattern that made very cold cloud tops over much of E CO. Over the Front Range however CTTs were not as cold. The CTTs over KDEN were near -5 °C to -15 °C. By 30/0300 UTC the low that was over extreme SE CO had moved into W KS. The coldest cloud tops still were over much of E CO. Over the Front Range the CTTs were variable between 0 °C to -20 °C. At KDEN the temperature dropped from 43 °F to 28 °F. No precipitation was reported. Visibility was 10 mi over the time period. Winds were from the S/SE at 5 to 10 kt. Cloud base heights were between 11000 and 20000 ft AGL. Pressure climbed slightly from 984 mb to 986 mb.

0600 UTC to 1200 UTC

At 30/0600 UTC the low over Western SD was nearly stationary. Another low had pushed southward into Southern WY. The coldest cloud tops were still over E CO. CTTs over KDEN were between -5 °C to -15 °C. By 30/0900 UTC the low over Southern WY had pushed into Central/northern CO. The low in Western KS had slightly pushed northeast. Colder clouds had moved over the Front Range. The CTT over KDEN was near -45 °C. At KDEN the temperature rose from 28 °F to 32 °F. The visibility was 10 mi for the entire time period. Winds were from the S/SE between 5 and 10 kt. Cloud base heights were variable from 8000 to 20000 ft AGL. Pressure dropped then slightly rose to 987 mb.

1200 UTC to 1800 UTC

At 30/1200 UTC the low in Central/northern CO remained stationary. This low and the low in central KS were associated with a cold front that had begun to push into CO at 30/1200 UTC. In addition another low moved near the CO-UT border which was associated with a stationary front over the mountains of W CO. Along the Front Range and through E CO along the Palmer Divide a trough of low pressure developed. Cold cloud tops were still over the Front Range. The CTT over KDEN was around -35 °C. By 30/1500 UTC the low in central/northern CO had moved southwest. The cold front had passed through Denver and CTTs were warming over the Front Range. At KDEN the temperature dropped from 32 °F to 24 °F. Light snow was reported from 30/1300 UTC to 30/1400 UTC and from 30/1700 UTC to 30/1800 UTC. Visibility was 10 mi until 30/1400 UTC when visibility dropped to 6 mi. Visibility then diminished again at 30/1700 UTC and remained between 1 and 3 mi for the rest of the day. Winds began to back over this time period. At 30/1200 UTC winds were from the SE at 10 kt. By 30/1800 UTC winds were from the NE at 15 kt. This was suggestive of the polar airmass moving into CO. Cloud base heights continued to decrease until at 30/1700 UTC the cloud base heights were 600 ft AGL. Pressure rose from 987 mb to 996 mb over the time period.

1800 UTC to 2400 UTC

At 30/1800 the low that was in western/central CO had intensified to a central low pressure of 982 mb. In addition a low formed in south/central CO with a central pressure of 988 mb. At this time the cold front had already made its way through KDEN. Cloud top temperatures over KDEN warmed and were near -15 °C. By 30/2100 UTC a “double-barrel” low formed over the western half of CO. This upward vertical motion provided by the low created clouds and cooled them considerably. The CTT over KDEN at this time was between -30 °C and -40 °C. At KDEN the temperature dropped from 24 °F to 13 °F. Light snow was reported over the time period. Winds were from the northeast between 10 and 15 kt. Cloud base heights were between 800 and 1300 ft AGL. Pressure rose from 996 to 998 mb.

Upper Air

At 30/0000 UTC at 250 mb a large trough was over the Intermountain West and Pacific Northwest. A fairly large ridge was in place over the Southern and Central Plains. A 100 kt jet streak was over much of western CO. At 500 mb the trough over the Intermountain West and Pacific Northwest was further west than the depicted at 250 mb. A small ridge was over the Southern Plains while a shortwave trough was over much of the Mississippi Valley. At 700 mb a substantial long wave trough was over much of the western US. There were two short waves embedded in the long wave.

At 30/1200 UTC at 250 mb the trough had dug substantially southward. The trough was over much of the western United States and had a 100 kt jet streak over eastern CO. CO was not in a very identifiable area of upper level divergence nor convergence. At 500 mb the trough was over the Intermountain West region and did not have a significant tilt. At 700 mb a the trough was very large and was further east than at 500 and 250 mb. Three shortwaves were embedded inside this trough.

Soundings

30/0000 UTC KDNR sounding: from the surface to 250 mb the sounding was dry. The freezing level was at 690 mb. From the surface to 790 mb winds were from the northeast at 5 to 10 kt. Above 790 mb winds backed and at the 625 mb level and above winds were from the SW/W and increased in speed with height.

30/1200 UTC KDNR sounding: from the surface to 600 mb the sounding was dry. From 600 to 400 mb the layer was saturated. The freezing level was at 742 mb. Winds were variable from the surface to 550 mb. Above 550 mb winds were from the S/SW and increased in speed with height.

Best Icing Time Periods: 30/1532 and from 30/2050 UTC through 30/2100 UTC.

Data Availability

PIREPs: 2 PIREPs within a 60-km radius of Platteville site.
CHILL: PPI's and RHI's from 30/2051 UTC through 30/2100 UTC.
Note that RHI's are only good if the azimuth is facing 190 degrees.
NIRSS: All NIRSS data present except for radar data on this day.

10 January 2011

Significant Weather Features:

Surface/Meteogram

0000 UTC to 0600 UTC

At 10/0000 UTC two inverted troughs were near the Central Plains/Central Rocky Mountain regions. One inverted trough was over central CO while the other was over central NE and central SD. An area of clouds was over KDEN at this time. This was caused by an upslope wind regime over the eastern plains of CO. In addition high pressure was building into the region as a continental polar airmass pushed southward across the region. The CTTs were between -30 °C and -45 °C. By 10/0300 UTC the inverted trough over central CO became more pronounced while the other inverted trough over the Central Plains had begun to propagate to the northeast. Clouds were thickening over the Front Range communities with CTTs over KDEN near -40 °C. At 10/0000 UTC at KDEN the temperature was 20 °F and dropped to 12 °F by 10/0600 UTC. Light to moderate snow was reported over the time period. At 10/0000 UTC 0.06 in of precipitation was reported. At 10/0600 UTC 0.11 in of precipitation was reported. Visibility was limited from 0 to 3 mi over the time period. Over the time period winds were from the ENE at 5 to 10 kt. Cloud base heights were variable over the time period between 700 and 2100 ft AGL. Pressure rose from 1011 mb at 10/0000 UTC to 1018 mb by 10/0600 UTC.

0600 UTC to 1200 UTC

At 10/0600 UTC the inverted trough was still over central CO with cloud tops cooling over KDEN. The CTT over KDEN was approximately -45 °C. By 10/0900 UTC the clouds were still in place but had warmed. The CTT over KDEN was near -35 °C. At KDEN the temperature dropped from 12 °F to 6 °F over the time period. Light snow was reported over the time period. At 10/1200 UTC 0.45 in of accumulation was reported. Visibility over the time period was at 1 mi. Winds began to back from the east to northwest by 10/1200 UTC. Wind speeds were between 5 to 15 kt. Cloud base heights were fairly consistent between 700 and 900 ft AGL. Pressure climbed from 1018 to 1023 mb over the time period.

1200 UTC to 1800 UTC

At 10/1200 UTC a center of low pressure had developed over central/eastern NE which was associated with the inverted trough over the Central Plains. In central CO the inverted trough was still in place. CTTs over KDEN had warmed slightly to a temperature near -30 °C. By 10/1500 UTC the clouds had begun to clear out of the region. The CTT over KDEN at this time was approximately -25 °C. At KDEN the temperature had cooled to near 1 °F by 10/1600 UTC but had warmed slightly after this time to 7 °F by 10/1800 UTC. Light snow was reported until 10/1400 UTC. At 10/1500 UTC haze was reported. By 10/1800 only 0.01 in of precipitation was reported. Visibility began to climb from 1 mi at 10/1200 UTC to 10 mi by 10/1800 UTC. Winds continued to back. Winds at 10/1200 UTC were from the northwest at 5 kt. By 10/1800 UTC winds were from the SE at 5 kt. Cloud base heights were also more elevated over the time period. Pressure slightly rose to 1025 mb by 10/1800 UTC.

1800 UTC to 2400 UTC

At 10/1800 UTC clouds had significantly cleared. According to the IR satellite image over KDEN the CTT was at -10 °C. By 10/2100 UTC the inverted trough was still over Central CO, however significant cold topped clouds were not over the Front Range communities. At KDEN the temperature increased slightly then dropped to 5 °F by 10/2300 UTC. No precipitation was reported over this time period. Visibility remained at 10 mi. Winds were from the east-southeast at 5 kt. Cloud base heights were higher and remained at 14000 ft AGL by 10/2000 UTC. Pressure also slightly increased to 1028 mb.

Upper Air

At 10/0000 UTC at 250 mb a negatively tilted trough with an associated cut off low was making its way through the Rocky Mountain/Plains regions of the United States. A jet maximum of 125 kt was located over a large portion of the Intermountain West. CO was not affected by this jet maximum. At 500 mb the closed low was over MT with a large trough visible over the Plains regions of the United States. At 700 mb the closed low is not detectable; nevertheless a trough is noticeable over the Plains region.

At 10/1200 UTC at 250 mb the closed low had moved into eastern MT. The associated trough was still over the Plains region of the United States. The jet maximum had slightly moved towards the SE and part of the maximum was over SW CO. At 500 mb the closed was over E MT with the associated trough over the Central Rockies and Plains regions. At 700 mb there are two shortwave troughs embedded in a long wave. One shortwave stretches southward from the Northern Plains along the lee-side of the Rocky Mountains. The second shortwave stretches from the Central Plains into the Lower Mississippi Valley.

Soundings

10/0000 UTC KDNR sounding: a saturated layer existed from the surface to ~ 425 mb. The CTT was around -38 °C. The freezing level on the sounding was below ground. Winds from the surface to 650 mb were from the northeast between 5 and 10 kt. From 650 mb and aloft winds were from the southwest/west and increased in speed with height.

10/1200 UTC KDNR sounding: (note the sounding dew point calculation was not available after 580 mb) a saturated layer existed from the surface to ~ 580 mb. The freezing level was below ground. From the surface to 650 mb the winds were from the north/northwest at 10 kt. Above 650 mb the winds back and are from the west/southwest and increase in speed with height.

Best Icing Time Periods: 10/0000 UTC through 10/0330 UTC

Data Availability

PIREPs: 2 PIREPs within a 60-km radius from Platteville site.
CHILL: CHILL initiates radar at 10/0051 UTC.
Good PPI's: 10/0053 UTC, 10/0100 UTC, 10/0253 UTC.
Good RHI's: 10/0051 UTC, 10/0059 UTC, 10/0259 UTC.

PPI's and RHI's are only good if the azimuth is pointing towards ~190 degrees +/- 20 degrees.
NIRSS: **Ka-Band Radar missing.**

19 January 2011

Significant Weather Features:

Surface/Meteogram

0000 UTC to 0600 UTC

At 19/0000 UTC the Front Range communities were under the periphery of high pressure to the west over Central UT. A stationary front stretched from Southwestern KS into Western NE, Central WY and through Central ID where a center of low pressure was located. Over the next 6 hours a lee-side trough would develop east of the Front Range Mountains of CO. At 19/0000 UTC the CTT over the KDEN was between -55 °C and -60 °C. At KDEN the temperature had slowly dropped from 42 °F to 36 °F by 19/0600 UTC. Visibility was 10 mi for this time period and winds were from the southeast until 19/0600 UTC when winds veered from the southwest. Pressure over this time period increased from 1011 to 1013 mb and then decreased to 1008 mb.

0600 UTC to 1200 UTC

At 19/0600 UTC a lee-side trough had developed east of the Front Range. This lee side trough was associated with two lows in CO. One low was over North-Central CO and the other low was over extreme Southeastern CO. CTTs were fairly warm over KDEN at around -15 °C. By 19/0900 UTC the two lows had remained nearly in the same area and CTTs over KDEN had warmed to -5 °C to -10 °C. By 19/1200 UTC the lows had remained again in the same area as 0600 UTC, however clouds began to thicken and cool near the KDEN area. CTTs over KDEN were between -30 °C and -40 °C. At KDEN temperatures over this time period cooled from 36 °F to 27 °F. Visibility was at 10 mi from 19/0600 UTC to 19/1100 UTC. At 19/1200 UTC the visibility had reduced down to 1 mi. Winds were variable over this time period but were light between 5 and 10 kt. Pressure had decreased from 1008 to 1007 mb.

1200 UTC to 1800 UTC

At 19/1200 UTC the two lows were still in place over North-Central CO and extreme Southeastern CO. By 19/1500 UTC the low over North-Central CO had moved south and was located over Fort Collins. Clouds began to build over KDEN by 19/1500 UTC. The CTTs were between -30 °C and -40 °C. By 19/1800 UTC the low that was over North-Central CO had propagated towards the west over the mountains. The low in extreme Southeastern CO had moved southward into the Northern part of the TX Panhandle. CTTs over KDEN at 19/1800 UTC were between -15 °C and -30°C. At KDEN the temperature over this time period slowly climbed from 27 °F to 34 °F. Visibility at 19/1200 and 19/1300 UTC was very low near 1 mi and gradually increased to 10 mi by 19/1600 UTC. Winds at 19/1200 UTC were from the west-southwest at 5 kt and veered from the northwest at 5 kt by 19/1800 UTC. Cloud base heights dropped significantly at the beginning of this time period (200 ft AGL) and increased 15,000 ft AGL by 19/1800 UTC. Pressure remained near 1007 mb for this time period.

1800 UTC to 2400 UTC

At 19/1800 UTC there was a low pressure over central CO. By 19/2100 UTC the low had remained fairly stationary while a stationary front formed connecting the low in central CO to the low in NE NM. Clouds also began to build into the Front Range region. CTTs over KDEN at 19/2100 UTC were between -30 °C to -35 °C. At KDEN the temperature climbed gradually from 34 °F at 19/1800 UTC to 40 °F by 19/2000 UTC. After 19/2000 UTC the temperature quickly dropped and was at 18 °F by 19/2300 UTC. Light to moderate snow was reported from 19/2200 UTC to 19/2300 UTC. Visibility at 19/1800 UTC was at 10 mi. At 19/2200 UTC the visibility dropped to 2 mi and by 19/2300 UTC the visibility dropped to zero. At 19/1800 UTC the winds were from the northwest at 5 kt. The winds veered slightly from the north by 19/2100 UTC and were strong between 20 to 25 kt. Cloud base heights from 19/1800 UTC dropped to 800 ft AGL by 19/2200 UTC. From 19/1800 UTC pressure slightly decreased to 1005 mb at 19/2000 UTC then increased to 1017 mb by 19/2300 UTC.

Upper Air

At 19/0000 UTC a very evident positively-tilted trough is noticeable in the flow across the Mississippi Valley with a 125-kt jet streak over much of CO. CO was also underneath an area of divergence aloft At 500 mb the positively-tilted trough is clearly evident. In addition a very small shortwave is visible east of the Front Range. At 700 mb the trough is visible over the Mississippi Valley with a small shortwave embedded in the flow over the Central Rockies.

At 19/1200 UTC at 250 mb the flow over CO has become very zonal and the trough that was over the Mississippi Valley at 19/0000 UTC is now over the Atlantic States. Additionally another positively tilted trough is over the Intermountain West. At 500 mb the flow over CO is zonal however the large trough that is perceptible at 250 mb is not as prominent at 500 mb. At 700 mb a lee-side trough is embedded in the flow east of the Front Range in CO. The positively tilted trough that is at 250 mb over the Intermountain West is obvious at 700 mb, while the trough over the Atlantic States was hardly evident.

Soundings

19/0000 UTC KDNR sounding: from the surface to approximately 520 mb there is a dry layer. From 520 mb to 340 mb (where the soundings dew point calculation is last correct) there is a saturated layer. The freezing level was at 732 mb. From the surface aloft the winds are stay fairly consistent from the W/NW with increasing speed aloft.

19/1200 UTC KDNR sounding: there was a small saturated layer from the surface to about 790 mb. The freezing level was below ground. A large inversion was in place atop this saturated layer. This could be suggestive of freezing/frozen precipitation in the lowest layer of the atmosphere. Winds at the surface were from the NW at 5 kt and backed from the west as the sounding went aloft Winds also increased in speed the higher the sounding went.

Best Icing Time Periods: 20/0006 UTC

Data Availability

<u>PIREPs:</u> One PIREP within a 60-km radius of Platteville site.
<u>CHILL</u>:
RHI's at 19/2358 UTC and 20/0007 UTC.
PPI at 20/0008 UTC.
<u>NIRSS:</u> No Radar data for day. Need to check.

31 January 2011

Significant Weather Features

<u>Surface/Meteogram</u>

0000 UTC to 0600 UTC

At 31/0000 UTC a stationary front was set up along the Front Range suggesting the beginning of a cold air damming event with weak easterly upslope taking place throughout the rest of the day. Two lows were positioned along the stationary front, one in South/Central WY and the other in South/Central CO. Cold air damming is suggestive in this situation as an extensive cloud deck is noticeable east of the Front Range. The temperature had slowly dropped from 36 °F to 24 °F by 0500 UTC. The only weather obscuration reported during this time period was fog and haze at 0500 and 0600 UTC. The visibility dramatically dropped from 10 mi to zero over this time period.

0600 UTC to 1200 UTC

At 31/0600 UTC clouds east of the Front Range were receding towards the Eastern Plains of CO. As time went onwards near 1200 UTC clouds reformed east of the Front Range and the stationary front had moved into the Central Mountains of CO. In addition the low in south/Central WY had disappeared and reformed by 1200 UTC. Fog and haze were reported during this time period and visibilities had also dropped to 0 mi at KDEN. The temperature had slowly dropped to 24 °F and stayed steady in the mid to upper 20's over the time period. Pressure also slowly began to rise as cold air had built in from the NNE.

1200 UTC to 1800 UTC

At 31/1200 UTC clouds east of the Front Range were cold with top temperatures near -55°C. As time progressed towards 1800 UTC the stationary front remained in place as the cloud top temperatures warmed. Clouds began to thin out later in the time period. Temperatures also began to drop from 24 °F to 8 °F. Haze was reported from 1200 o 1300 UTC. Light snow was reported at 1400 UTC. At 1500 UTC light freezing rain was reported. From 1600 to 1800 UTC light to moderate snow was reported. Visibility remained very low between 0 and 1 mi over the time period. Winds also began to veer over this time period. Pressure increased from 1015 to 1024 mb as the arctic airmass had made its way into CO.

1800 UTC to 2400 UTC

At 31/1800 UTC cold air damming was clearly visible along the Front Range. Cloud tops were still fairly cold near -30 °C to -40 °C. By 2100 UTC a new low formed in the West Central region of CO. Temperatures stayed steady around 8 °F until 2300 when the temperature began to cool to 6 °F. Light to moderate snow and haze were reported over the time period. Visibilities remained between 0 and 1 mi. Pressure slightly decreased around 2100 UTC suggesting a secondary cold frontal passage as pressure rose slightly after this drop.

Upper Air

At 31/0000 UTC at 250 mb a large positively tilted trough is noticeable in the flow over the Intermountain West states with a small ridge in place over the Southern/Central Plains region of the US. At 500 mb the trough is still distinct while the small ridge is not as pronounced. At 700 mb a lee side trough is evident over the eastern plains of CO.

At 31/1200 UTC at 250 mb the trough has become very positively tilted over the Intermountain West states. At 500 mb this trough is visible in the flow with a ridge of high pressure over the Mississippi Valley and Ohio Valley. At 700 mb two troughs are embedded in the flow, one that extends from Central Wyoming southwestward into southwestern Arizona. The other trough outspreads from ND into Central OK.

Soundings

31/0000 UTC KDNR sounding: a small saturated layer exists from 550 mb to 460 mb. The freezing level was at 698 mb. Winds from the surface to 650 mb veer from the NE to the W. Above 650 mb winds remain from the W/SW through the rest of the sounding.

31/1200 UTC KDNR sounding: a saturated layer was seen from the surface through 740 mb. The freezing level is below ground. Winds at the surface are from the NE at 5 kt and back towards the W at 725 mb. From 725 mb winds remain from the W/SW.

Best Icing Time Periods: 31/1320 UTC through 01/0240 UTC

Data Availability

PIREPs: 23 PIREPs within a 60 km radius from Platteville site.
CHILL: Not available
NIRSS: All NIRSS data present except for radar data.

7-8 March 2011

Significant Weather Features

Surface/Meteogram

0000 UTC to 0600 UTC

At 07/0000 UTC a continental polar air mass was moving southward along the Front Range. An area of low pressure was set up over S CO with a trough of low pressure extending eastward into the areas of the OK Panhandle, extreme SW KS and extreme SE CO. An additional area of low pressure was situated over south-central WY. A large cloud shield was in place over much of CO with CTTs over KDEN around -38 °C to -48 °C. A small anticyclonic upslope regime was in place at this time. The temperature at 0000 UTC was at 43 °F and decreased to 30 °F by 0600 UTC. No precipitation was reported from 0000 to 0400 UTC. After 0400 UTC to 0700 UTC light snow was reported at KDEN. Precipitation at 0600 UTC totaled 0.04 in. Visibility from 0000 to 0400 UTC was at 10 mi. After 0400 UTC the visibility dramatically decreased to 1 mi at 0400 UTC and remained between 1 and 7 mi for the rest of the day. Winds between 0000 to 0400 UTC were from the NE between 5 and 15 kt and veered from the E between 0500 to 0600 UTC. Cloud base heights dropped from 8000 ft AGL at 0000 UTC to 400 ft AGL by 0600 UTC. MSLP slightly increased from 1006 mb to 1007 mb over this time period.

0600 UTC to 1200 UTC

At 07/0600 UTC clouds were beginning to reduce in coverage over NE CO. The cold front had slowly moved south. The low over south-central WY moved into Northwestern CO. The low that was over S CO had moved over SE CO/NE NM and deepened to a central pressure of 1001 mb. The CTT over the Front Range was variable between -20 °C and -40 °C. The temperature at 0600 UTC was at 30°F and dropped down to 21 °F by 1200 UTC. Between 0600 and 0700 UTC light snow was reported at KDEN. Between 0900 and 1200 UTC haze and fog were reported. Precipitation amount at 1200 UTC was at 0.05 in. Visibilities remained low between 0 and 3 mi. Winds between 0600 and 1200 UTC were from the N and E with a constant speed of 10 kt. Cloud base heights were low over this period between 100 and 400 ft AGL. MSLP rose from 1007 mb at 0600 UTC to 1010 mb at 1200 UTC.

1200 UTC to 1800 UTC

At 07/1200 UTC clouds were warmer over this period which suggested lower cloud tops. The cold front dived further south into SE CO. One low formed over NE NM with a central pressure of 1001 mb and another was over the panhandle of OK with a central pressure of 1002 mb. The temperature at 1200 UTC was at 21 °F and dropped to 20 °F by 1800 UTC. Both haze and fog were reported over this time period with visibilities between 0 and 3 mi. Winds were from the E over this period with speeds between 5 and 10 kt. Cloud base heights were low between 100 and 300 ft AGL. MSLP rose from 1010 to 1012 mb during this time period.

1800 UTC to 2400 UTC

At 07/1800 UTC the cold front had moved south into the northern part of the TX panhandle and NE NM. Clouds were visible in S CO on the IR image while lower topped clouds were in place over NE CO. Three lows were developing along/near the cold front. One was over NE NM, the second was over the TX panhandle and the third was over the OK panhandle. The temperature slightly increased during this time period from 20 °F to 24 °F. Haze was reported between 1800 and 2200 UTC. Visibility increased from 3 to 7 mi. Winds remained out of the E with speeds between 5 and 10 kt. Cloud base heights increased from 300 to 1100 ft AGL by 2300 UTC. MSLP dropped during this time period from 1012 to 1008 mb.

Upper Air

At 07/0000 UTC at 250 mb the flow was very zonal with diffluence evident over the Central and Southern Plains. Wind speeds over CO were between 100 and 125 kt. A small trough was noticeable over the Pacific Northwest. At 500 mb the flow looked identical to the 250 mb flow with a zonal pattern and the presence of a trough over the Pacific Northwest. A small shortwave was present over the Rocky Mountains at this time. At 700 mb an isothermal ridge was in place over the Front Range. A shortwave was present also.

At 07/1200 UTC at 250 mb the flow was zonal with a jet maximum over SE CO with 150 knot winds. This placed SE CO in the left exit region of the jet maximum which identifies why surface lows were forming near SE CO/NE NM. Moreover the trough over the Pacific Northwest had moved over the Intermountain West states and had a slight negative tilt. At 500 mb the flow was zonal and had two shortwaves embedded in the flow. One shortwave was over the Northern/Central Plains and the other was over the Southern Plains/Lower Mississippi Valley. The trough that was previously over the Pacific Northwest had made its way into the Intermountain West states. At 700 mb a large wave was in place over the lee side of the Rocky Mountains with another large wave in place over the Intermountain West states. The isothermal ridge was not present at this time.

Soundings

07/0000 UTC KDEN sounding: a saturated layer was present from the surface to ~ 675 mb. The CTT was around -8 ° C. The freezing level on the sounding was at 743 mb.Winds from the surface to 750 mb were from the NNW and sharply veered from the SW at 725 mb. Above 725 mb winds were from the WSW and speeds increased with height up to 200 mb.

07/1200 UTC KDEN sounding: a saturated layer existed from the surface to ~700 mb. The CTT was around -9 °C. The temperature at the surface cools from -6 °C to -9 °C at the top of the cloud. This suggests a stable cloud layer where supercooled drops could form. Winds from the surface to 800 mb were very light at 5 kt from the east-northeast. At 775 mb winds are from the northwest at 5 kt and remain from the west-northwest throughout the sounding.

Best Icing Time Periods: 07/0200 UTC through 07/0400 UTC, 07/1300 UTC through 07/1500 UTC, 07/1930 UTC through 08/0300 UTC.

Data Availability

PIREPs: 25 PIREPs within a 30-km radius of Platteville site.
CHILL: CHILL initiates radar at 07/1723 UTC.
Good PPI's: from 07/1723 UTC through 07/2345 UTC.
Good RHI's: from 07/1736 UTC through 07/1922 UTC, 07/2110 UTC through 07/2149 UTC, 07/2257 UTC through 07/2344 UTC.
PPI's and RHI's are only good if the azimuth is pointing towards ~190 degrees +/- 20 degrees.
NIRSS: All NIRSS data present.

12 May 2011

Significant Weather Features

Surface/Meteogram

At 12/0000 UTC a low pressure system was setup over extreme northwestern KS. A small cold front extended behind the system along the NM, OK panhandle/CO border. On the IR satellite image this extra-tropical cyclone (ETC) can be seen across much of the Central US. Over the Front Range fairly high cloud tops are shown with CTTs of ~ 40 °C to -50 °C. At this time MSLP was fairly high at KDEN (1012 mb). Winds from 0000 to 0600 UTC were northerly at 15 kt. From 0000 to 0100 UTC moderate rain was reported at KDEN. From 0200 to 0300 UTC moderate snow was reported at KDEN. From 0300 to 0600 UTC light snow was reported at KDEN. Temperatures dropped from the upper 30s at 0000 UTC to low 30s by 0600 UTC. Cloud bases were very low over this time period from 400 to 1000 ft AGL. Consequently visibilities were also very low (0 to 10 mi).

At 12/0600 UTC the low pressure center continued to move off towards the northeast. At this time the cold front plunged into extreme NE NM and the OK/TX panhandles. High pressure was continuing to build in over CO. An extensive cloud mask was still over NE CO with CTTs between ~ 40 °C to -50 °C. Temperatures were steady in the low to mid 30s. Precipitation switched between periods of light rain to light snow from 0600 to 1000. From 1000 to 1200 UTC moderate rain was reported. Cloud bases began to slightly rise and were between 500 ft AGL to 1600 ft AGL. Winds were from the north/northwest between 10 and 15 kt. Visibilities slightly increased during the time period from 0600 to 1200 UTC.

At 12/1200 UTC the surface low continued to move northeast and was in south/southwestern NE. Cold air behind the front had made its way through NM and the TX/OK panhandles. Over the Front Range was a mix of CTTs ranging from -10 °C to -35°C. The temperature began to rise from the mid 30s into the lower 40s from 1200 to 1800 UTC. Light rain was falling at KDEN from 1200 to 1800 UTC. Winds had a northerly component with speeds between 10 and 15 kt. MSLP began to rise rapidly from ~ 1015 mb at 1200 UTC to 1018 mb at 1800 UTC. Cloud bases were between 1000 to 2600 ft AGL from 1200 to 1800 UTC.

At 12/1800 UTC the surface low was in position over south central NE. A widespread cloud mask was still over CO at this time. CTTs over the Front Range were between -35 °C and -40 °C with warmer cloud tops over the Eastern Plains. From 1800 to 2400 UTC MSLP slightly increased to from 1018 mb to 1020 mb. Light rain continued to fall over KDEN over this time period. Winds had a NNW component between 10 and 15 kt. Cloud bases were lower over the time period from 1800 to 2400 UTC with heights between 1100 and 1600 ft AGL. Temperature increased from 40 °F at 1800 UTC to 45 °F at 2400 UTC.

Upper Air

At 12/0000 UTC at 250 mb a fairly large negatively-tilted trough was over the Rocky Mountains. CO was at the bottom of this upper level trough. Over the Central and Northern Plains was a jet streak with a maximum of 100 kt north of the ND border. At 500 mb the trough axis was over central CO. At 700 mb the low was centered over eastern CO with wrap around moisture in NE CO. The -4 °C isotherm was atop KDEN.

At 12/1200 UTC at 250 mb the upper level trough was losing its negative tilt. The trough axis was now positioned over eastern CO, WY, and MT. The center of circulation was over extreme northeastern CO. At 500 mb the trough axis was above the CO/KS border. The winds over KDEN were from the northwest at 50 kt. At 700 mb the low was atop extreme northeastern CO, SW NE and NW KS. Additional wrap-around moisture was making its way into NE CO at 700 mb. KDEN was still under the -4 °C isotherm.

<u>Soundings</u>

12/0000 UTC sounding: a saturated layer was in place from 801 mb to ~ 650 mb. The CTT was around -8 °C. The freezing level was at 782 mb. From the surface to 650 mb winds were from the NE between 5 and 20 kt. At 600 mb the winds backed from the SE. Winds continued to back aloft until 300 mb where winds became S/SE for the rest of the sounding.

12/1200 UTC sounding: a saturated layer was shown from the surface to approximately 500 mb. The CTT was ~ 18 °C. The freezing level for this sounding was at 785 mb. Winds between the surface and 100 mb had a northerly component. From 100 mb for the rest of the sounding winds were from the SE.

Best Icing Time Periods: 12/0155 UTC, 12/1357 UTC, 12/1645 UTC

Data Availability

<u>PIREPs:</u> Four PIREPs within a 30-km radius of Platteville site.
<u>CHILL:</u> CHILL initiates radar at 12/1134 UTC.
Good PPI's: from 12/1134 UTC through 12/2310 UTC.

Good RHI's: from12/1134 UTC through 12/2100 UTC
PPI and RHI Images are saved in this document from the best icing times
Note All other RHI figures are on the VCHILL server for this day.
<u>NIRSS:</u> No data are present for this day.

15 May 2011

Significant Weather Features:

<u>Surface/Meteogram</u>

At 15/0000 UTC an area of clouds with CTTs of near -50 °C was over northeastern CO. High pressure was dominant over the region as a continental polar air mass moved southward out of Canada. At this time temperatures were in the upper 40s with winds out of the north at 5 kt. Pressure was still rising at this time. Between 0100 and 0400 UTC light rain fell at KDEN due to an upslope regime. Cloud bases were between 2000 to 4400 ft AGL from 0000 to 0600 UTC.

At 15/0600 UTC clouds were becoming thinner on IR satellite. CTTs over the Front Range were around -35 °C. Pressure slightly begins to fall between 0600 and 1200 UTC but rises again after 1200 UTC. Cloud base heights were between 2000 and 3400 ft AGL from 0600 to 1200 UTC. Winds over this time period were from the E at 10 kt.

At 15/1200 UTC clouds again were thinning out on the IR satellite image. CTTs over the Front Range were around -15 °C. Pressure began to rise slightly and winds began to slightly veer from 1200 to 1800 UTC. Cloud base heights were between 1700 and 2900 ft AGL. Additionally temperatures were beginning to rise out of the upper 30s into the lower 40s between 1200 and 1800 UTC.

At 15/1800 UTC clouds were of stratiform appearance on the IR satellite image. In the mountains of CO a tighter pressure gradient began to form as lower pressure neared the state from the west. Pressure began to fall over the next 6 h. The cloud base heights remained very level between 2200 to 3000 ft AGL between 1800 and 2400 UTC. Temperatures climbed into the upper 40s.

Upper Air

At 15/0000 UTC flow was very zonal across much of the western and central plains states. A deep trough is noticeable over the Pacific Ocean near the Pacific Northwestern states. At 500 mb a ridge was obvious in the flow. At 700 mb the ridge was embedded in the flow over the southern plains, central plains and central Rockies. Isotherms show the progression of a continental polar air mass into parts of extreme southeastern CO and western KS. At 15/1200 UTC an upper level ridge starts to become more pronounced over UT, W/NW CO, and WY. The upper level trough near the Pacific Northwest was beginning to dig and become negatively tilted. Strong diffluence was over northeastern Nevada, with a jet streak over central/southern California and central Nevada. At 500 mb the ridge was still in the flow over the southern Rockies, southern plains, and most of CO. At 700 mb the ridge was still noticeable over the southern plains, southern Rockies and southern CO. Cold air dipped southward into northeastern NM and the OK panhandle.

Soundings

15/0000 UTC sounding: dry air was in place from the surface to about 746 mb. From 746 mb to 625 mb there was a saturated layer with a CTT of ~ -7 °C. Winds from the surface to 725 mb were from the northeast. From 700 mb to the top of the sounding winds had a W/SW component. The freezing level according to this sounding was 771 mb.

15/1200 UTC sounding: a saturated layer started nearly from the surface (LCL of 810 mb) to approximately 650 mb. The cloud top temperature was ~ -5 °C. According to the sounding the freezing level was at 816 mb. Winds from the surface to 800 mb were light (5-10 kt) from the SE. Winds above 750 mb were from the SW with wind speed increasing with height.

Best Icing Time Periods: 12/1240 UTC through 12/1628 UTC

Data Availability

PIREPs: 7 PIREPs within a 30 km radius from the Platteville site

CHILL: CHILL initiates radar at 15/1911 UTC.
Good PPI's: from 15/1929 UTC through 15/2320 UTC.
Good RHI's: from 15/2022 UTC through 15/2315 UTC.
CHILL data does not match best times for icing.
NIRSS: No data present for this day.

19 May 2011

Significant Weather Features:

Surface/Meteogram

At 19/0000 UTC an area of low pressure was located in southeast CO. From this an occluded front extended northwest over the Sangre de Cristo Mountains in central/southern CO. Over NW CO another area of low pressure was in place. Extensive cloud cover could be seen over the Front Range with CTTs around -45 °C to -50 °C over KDEN. At KDEN light to moderate rain fell with temperatures in the middle 40s. Low visibilities were observed (0 to 5 mi) between 0000 and 0600 UTC.

At 19/0600 UTC the first low over SE CO had moved into the OK/TX panhandle region. An inverted trough extended northwest from this low over central CO to the other low located in northwestern CO. Most of CO was covered with clouds at this time. Between 0600 and 1200 UTC temperatures gradually fell into the upper 30s. The cloud bases were low from 1000 to 2000 ft AGL at KDEN amongst these times.

At 19/1200 UTC the low was still in place over northwest CO. The KDEN meteogram showed fog between 1200 and 1500 UTC with pressure gradually rising. Over the Front Range CTTs were between 0 °C and -10 °C. Between 1500 and 2000 UTC haze was observed at KDEN.

At 19/1800 UTC the low over NW CO was now located over central CO. The Front Range was still covered in a widespread layer of clouds. Cloud bases from 1800 UTC until the end of the day were between 1300 and 5000 ft. Thunderstorms began to develop off the Front Range and moved over the Eastern Plains by 2100 UTC and continued through 2200 to 2300 UTC.

Upper Air

At 19/0000 UTC at 250 mb a positively-tilted upper level trough was centered over the western United States. This upper level feature was associated with an extensive cloud cover over the Central Rockies, Central Plains, Northern Plains and the Great Basin. Over central and eastern CO there was considerable diffluence. In addition, the left exit region of the jet streak was nearing southern CO. Lower in the atmosphere at 500 mb a closed low was above Nevada and UT. Diffluence was still noticeable at this level over the Central Plains region. Lower at 700 mb, an area of moisture was present over CO, with the 0 °C isotherm located atop KDEN.

At 19/1200 UTC at 250 mb the upper level trough was moving closer toward the Central Rockies. Diffluence was over the eastern plains of CO and parts of the Central Great Plains. The left exit region of the jet was additionally located over northern NM and southern CO. At 500 mb the closed low moved over eastern UT and western CO with diffluence over the Central Great Plains. At 700 mb an area of moisture was still in place over NE CO.

Soundings

19/0000 UTC KDEN sounding: a saturated layer was in place from ~ 725 mb to ~ 530 mb with a CTT of around -15 °C. The freezing level was at 700 mb for this sounding. At the surface winds were from the NE at 10 kt. At 750 mb winds are from the south-southwest at 10 kt. Throughout the rest of the sounding winds have a southwesterly to westerly component.

19/1200 UTC KDEN sounding: a moist layer was evident from the surface to 600 mb with a CTT of -11 °C with the freezing level at 724 mb . Winds throughout the entire sounding had a SE to SW component.

Best Icing Time Periods: According to the CIP meteogram the best icing time periods were between 19/1800 UTC and 19/2100 UTC where all the icing PIREPs occured. The greatest severity of icing reported on this day from all PIREPs was a category of light.

Data Availability

PIREPs: None
CHILL: CHILL initiates radar at 19/0001 UTC and runs through 19/2302 UTC.
Good PPIs: from 19/0001 UTC through 19/2302 UTC.
Good RHIs: from: 19/2205 UTC through 19/2210 UTC.
Note: the only RHIs from this day are labeled test RHIs on Virtual CHILL. Also, these RHI's had an azimuth of 116° and 117°, which are not facing the Platteville site directly. Platteville is at 190° Azimuth from the CHILL radar.
NIRSS: **NIRSS data are missing for this day.